Monatshefte für Chemie - Chemical Monthly (2020) 151:649–675
https://doi.org/10.1007/s00706-020-02590-w

REVIEW

Fischer–Tropsch synthesis, the effect of promoters, catalyst support, and reaction conditions selection

Jan Horáček[1]

Received: 7 November 2019 / Accepted: 27 March 2020 / Published online: 6 May 2020

Abstract

This work brings the overview of Fischer–Tropsch synthesis (FTS) from catalysis point of view. The role of promoters' type and their amount loaded into the catalyst are described and discussed for both, iron- (Cu, K, Na, S, Zr, Ni) and cobalt (Ru, Pt, Re, Zr, Ag, Rh, Ir, Au)-based catalysts, respectively, as same as the role of catalyst supports and reaction conditions. Catalyst supports discussed in this work are from the group of oxides, mesoporous silicas and zeolites, carbon-based materials, and carbides. Reaction conditions studied and discussed are reaction temperature, gas hourly space velocity of syngas and hydrogen to carbon monoxide ratio in syngas and reaction pressure. For iron-based catalysts, reaction temperature is discussed in the range of 508–613 K, while for cobalt types in the range of 468–513 K. Reaction pressure is discussed for both catalyst types up to 3 MPa. All the parameters are presented and discussed using FTS selectivity to main groups of products, such as CH_4, CO_2, C_2–C_4 hydrocarbons, and C_{5+} hydrocarbons together with syngas conversion degree. Detailed review of data published in articles studying FTS over iron and cobalt catalysts supplied large data set for presenting and discussion of trends and effects of aimed parameters and for their visualization in form of set of charts. This data analysis brings complex overview of basic trends of catalytic properties of cobalt and iron catalysts.

Graphic abstract

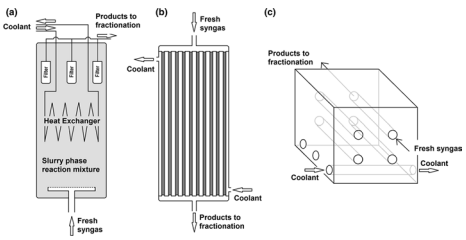

Keywords Fischer–Tropsch synthesis · Green chemistry · Heterogeneous catalysis · Hydrocarbons

Introduction

Fischer–Tropsch synthesis (FTS) represents universal reaction in processes for any organic matter transformation into hydrocarbons. The interest in this reaction increased in the first two decades of twenty-first century. The reason was worldwide effort to reduce production of greenhouse gases and their emission into the atmosphere. One of pathways how to reach this goal is the change of automotive fuels' composition. In Europe, automotive fuels have to contain renewable components as described by European directives (2009/28/EC, 2009/30/EC, RED II). Significant progress in these efforts was planned for year 2021. From this year, the contribution of first-generation biofuels (mainly fatty acids methyl esters, ethanol from food crops) has to be gradually reduced and contribution of advanced biofuels and second generation biofuels has to be implemented into automotive fuels. Advanced biofuels are typically produced from waste feedstocks, such as waste cooking oil/used frying oil or

✉ Jan Horáček
horacekj.unicre@seznam.cz

[1] Unipetrol Centre for Research and Education, Block 2838, 436 70 Litvínov-Záluží 1, Czech Republic

rendered fats without any other possible utilization in food industry. Fuels produced from these materials are typically fatty acid methyl esters (FAME) or Green diesel (also known as HVO—hydrotreated vegetable oil). Green diesel production is based on catalytic deoxygenation of feedstocks listed above into *n*-alkanes suitable for diesel fuel blending or further refining by hydroisomerization. Opposite to advanced ones, second-generation biofuels are produced from lignocellulose (waste wood, straw, etc.), or from municipal waste. While processes for advanced biofuels are technologically well described, processes for second-generation biofuels are still technically and economically problematic.

Initial treating of feedstocks for second-generation fuel production can be performed in two pathways: gasification of biomass (1) in defined amount of oxygen for syngas production, or pyrolysis (2) in absence of oxygen into liquid tar (so called bio-oil). The main advantage of gasification is production of relatively pure syngas, while bio-oil from pyrolysis is very unstable when exposed to light or high temperatures. Bio-oil can be used for syngas production by gasification in the same way as original feedstock. This makes sense for cost-efficient biomass (intermediate) transportation for longer distances for final treating by gasification and following processes. For efficient use of lignocellulose, this feedstock can be hydrolyzed prior to gasification or pyrolysis. Cellulose extracted by hydrolysis is suitable feedstock for fermentation into second-generation bioethanol. The solid residue from hydrolysis is still perspective feedstock for gasification or pyrolysis.

Primary products of lignocellulose or waste material treating cannot be used as automotive fuel components without any further treating. Bio-oil has to be stabilized prior to use in internal combustion engines by complicated hydrothermal processes using multistage catalytic hydrotreating using combination of catalysts (noble metals + sulfided [1–3]) or just sulfided catalysts in not isothermal reactor [4]. These processes are not available in commercial scale. The main problem of this stabilization step is rapid catalyst deactivation and coke formation. FTS transforms syngas from gasification into liquid products. This process is currently very well described with many industrial units installed. Syngas consists mainly of hydrogen, carbon monoxide, and carbon dioxide. Depending on the source of oxygen for gasification, significant amount of nitrogen can be present when air used for gasification. The reaction is based on interaction of H_2 and CO producing hydrocarbon chains as the main product, water as by-product, and reaction heat. In FTS, three basic reactions take place. These are "water gas shift" (WGS) where hydrogen is formed during interaction of CO and H_2O (1). This reaction is useful just in the case of proceeding syngas with low H_2:CO ratios, where WGS increases hydrogen content for hydrocarbons formation (2). Another important reaction is methanation, simple hydrogenation of CO or CO_2 into methane (3). This reaction is undesirable in processes focused on renewable fuels production. On the other hand, it is the key reaction in SNG (synthetic natural gas) production from biomass.

$$H_2O + CO \Leftrightarrow H_2 + CO_2 \quad \Delta H_R = -41\,\text{kJ/mol CO} \tag{1}$$

$$n\,CO + (2n + 1)\,H_2 \Rightarrow C_nH_{2n+2} + n\,H_2O \quad \Delta H_R = -156\,\text{kJ/mol CO}, \tag{2}$$

$$CO + 3\,H_2 => CH_4 + H_2O\ \Delta H_R = -209\,\text{kJ/mol CO}. \tag{3}$$

FTS main products are typically *n*-alkanes and α-olefins. The ratio of alkanes and olefin content decreases with enlarging hydrocarbons chains of organic product. As minor organic products, some branched hydrocarbons can be found. The waste aqueous phase contains some amount of oxygenated compounds. The selectivity of FTS to these compounds and their nature is given by the combination of catalyst and reaction conditions; nevertheless, these compounds are usually from group of alcohols and ketones [5].

Similar to hydrotreating of bio-oil, the FTS catalyst can be rapidly deactivated by interaction with reaction mixture. The risk of deactivation is in minor products of gasification, such as hydrogen sulfide, ammonia, hydro halogens, and aromatic compounds (BTX fraction, so called tars). These impurities have to be separated from syngas in multistage cleaning process with adsorbers and scrubbers. Content of sulfur-containing impurities (H_2S, COS, CS_2) has to be reduced to the concentration < 1 ppmv as same as nitrogen-containing impurities (NH_3, HCN) and hetero organic compounds. Content of hydrogen halides and alkali metals must be lower than 10 ppbv [6].

This work brings an overview of FTS catalysts, possibilities of their modification by promoters, and the role of reaction conditions in FTS.

FTS catalysts are usually sorted based on the main active metal in active phase. Ruthenium catalysts are known for their high stability and low deactivation rate. These catalysts are known for their high activity allowing operating FTS at relatively low temperatures in comparison with other catalysts types (approximately 450 K). Active phase can consist of ruthenium metal particles [7, 8], or it contains mixture of ruthenium and other metal, for example manganese [9, 10]. The most common catalysts in research publication and in industrial applications are cobalt catalysts. The main active centers are reduced metallic Co particles typically accompanied by not reduced oxide phase and mixed phases of cobalt and support [11–31]. The FTS reaction rate is proportional to reduced cobalt surface area. Similar to ruthenium

catalysts, cobalt type can be combined with manganese as well [32–35]. Cobalt catalysts provide adequate activity at temperatures around 490 K. The third and the oldest type are the iron catalysts. These are typical with their lower activity in comparison with ruthenium and cobalt types, which needs to be compensated by use of higher reaction temperatures above 520 K. The active phase consists of iron carbides [27, 36–44] and the main advantages of these catalysts are lower costs of active metal and promoters, higher stability, and ability to proceed CO rich syngas (H_2:CO below 2; vol.:vol.) long-term.

Ruthenium and cobalt catalysts are usually supported catalysts. In case of ruthenium it is mainly for high costs of active metal, while in the case of cobalt it is given by the effort to maximize surface area of reduced cobalt for maximizing the reaction rate. Porous catalyst supports are an efficient way for reaching high specific surface area and high surface of active phase, respectively. Activation of these catalysts is usually performed under temperature-programmed reduction in hydrogen. Cobalt can be activated also under hydrogen-rich syngas flow. Iron catalysts can be found in supported form as same as ruthenium and cobalt catalysts and in bulk/unsupported form as well. These catalysts can be activated by CO-rich syngas or by hydrogen. In the case of activation under hydrogen flow, the formation of carbide active phase takes place during initial stage of FTS.

Results and discussion

Catalysts promoters

For both main groups of catalysts, iron and cobalt types, catalyst promoters are frequently used and studied in research publications. These elements are typically used to modify some of active metal properties and properties of catalyst, respectively. Reasons for adding promoters to catalysts are lowering of necessary reduction (activation) temperature, modifying of FTS selectivity, catalytic activity increasing, and catalyst stability increasing. Last two reasons of promoters' use are closely connected with enlarging of lifecycle that plays an important role in process economy.

Cobalt catalysts

The most frequently used promoters of cobalt catalysts are noble metals. The main reasons for their application are lowering of temperature during activation procedure and increase of catalytic activity. Pt, Ru, Re, Ag, and Rh addition into catalyst can evoke significant lowering of necessary temperature during reducing of metal oxide into active metal particles. This promoting effect can be observed during activation of fresh catalysts as well as during activation of regenerated catalysts repeatedly after more regeneration cycles [45]. On the other hand, Ir and Au have tendencies to separate from cobalt active phase between single regeneration steps, thus catalysts promoted with these metals require increase of activation temperature after each regeneration cycle performed [45]. The effect of Ru in lowering of necessary activation temperature was well demonstrated with 9.5 wt% Co/γ-Al_2O_3 with Ru loading up to 1.0 wt% [46]. The Ru addition of 0.2 wt% significantly reduced the temperature of cobalt reduction from 770 K to approximately 620 K. Higher Ru loading did not lower temperature of reduction significantly. The observed temperature of cobalt for Ru loading of 0.5–1.0 wt% was approximately 600 K. The amount of Ru loading has to be carefully optimized regarding high costs of its precursors. Especially because at 0.5 wt% Ru loading, part of Ru formed separated metallic particles, which were not active in FTS (opposite to Ru catalysts). Catalyst with 0.2 wt% of Ru showed ruthenium-binding mostly in metallic particles with cobalt and partially at the surface of unreduced cobalt oxide particles. As described the Ru loading up to 1 wt% did not affect significantly CO conversion and selectivity to FTS products. The only effect was little increase in selectivity to olefinic compounds, which can be compensated by increase of reaction temperature from 463 to 483 K. In the case of SBA-15 supported catalyst, the presence of Ru promoter resulted in an increase of CO conversion and C_{5+} selectivity and lower selectivity to undesirable CO_2 and CH_4 [19]. Selectivity to C_2–C_4 products was not affected significantly (Fig. 1).

The effect of catalytic activity increase by promoters decreases in order Co–Pt > Co–Re > Co–Ru > Co. This comparison was described for 25 wt% loading of Co to La stabilized Al_2O_3 in fixed bed reactor [47]. Efficiency of promoter addition depends on few aspects, like the amount of promoter in active phase and method of promoter insertion. Significant differences in activity show catalysts prepared by one-step and multi-step loading of active metal and promoter(s). One-step procedure of inserting cobalt and promoters results in synthesis of catalysts with higher activity in comparison with catalyst prepared in two or more steps of active phase loading. This effect is very significant for Ru, where its loading in one step together with cobalt results in the case of Ru loading subsequently after cobalt. Similar effect can be reached with use of Pt and Re as promoters. The order of promoters' efficiency by reaction rate decreases in this way: Co–Pt > Co–Re > Co–Ru [48]. Turn over frequencies (TOF) of Pt, Re, and Ru catalysts was described as similar when using continuous stirred-tank reactor (CSTR), while Pd promoted catalyst showed 40% lower TOF. This was caused by Pd spreading on the surface of Co clusters and blocking their accessibility for reactants. As described in this study, the presence of Re and Ru promoters can increase selectivity of FTS to C_{5+} products and

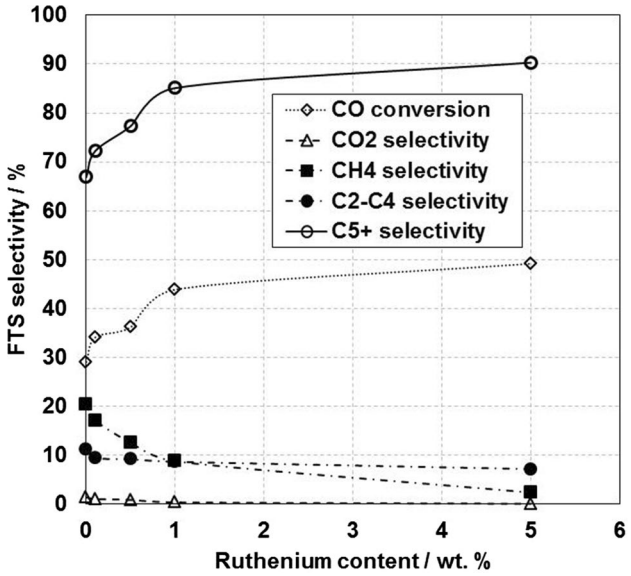

Fig. 1 Effect of Ru content in Co/SBA-15 catalyst; fixed-bed reactor, 493 K, 1.0 MPa, 3.6 $dm^3/g_{cat}/h$, 20% Co, H_2:CO = 2. Data from [19]

C_2–C_4 olefins accompanied by lower selectivity to 1-butene. The presence of Pt and Pd promoters reduces selectivity of olefinic compounds in general [11].

The combination of Ru for lowering activation temperatures with Pt for increasing catalyst activity seems to be perspective in development of cobalt catalysts. Moreover, both these promoters are able to significantly slow down cobalt reoxidation, which occurs during interaction of cobalt-active particles with oxide catalyst supports during FTS. Phenomenon of cobalt reoxidation gets more significant with raising partial pressure of water produced from FTS. The side effect of Ru and Pt presence in catalysts is lower stability of small cobalt particles, which disappear by sintering [49]. In comparison of Ru and Pt promoters, Pt has higher ability to slow down catalyst deactivation caused by formation of polymeric carbon [50].

Zirconium as promoter little modifies FTS selectivity on behalf of liquid C_{5+} products and inhibiting of WGS reaction and methanation. Significant suppression of methanation can be reached by addition of 1 wt% of Zr into the catalyst [26]. Another increasing of Zr content does not affect methanation, while WGS reaction rate was still decreasing. These trends were observed in short-term and long-term reaction as well (Fig. 2).

Iron catalysts

These catalysts are specific for use in high-temperature FTS. Promoters are used for stabilization of catalysts and increasing of their activity. The most common promoters are K and Cu. Direct comparison of these promoters in supported catalyst in fixed bed reactor shows decreasing catalytic activity and selectivity to olefins in order Fe–K > Fe–Cu > Fe (SBA-15 supported). Contribution of SBA-15 as catalytic support is its ability to reduce methanation and to increase yield of C_{5+} fraction [51].

Potassium addition to catalyst evokes decrease of CO conversion with increasing K:Fe ratio in fixed bed reactor

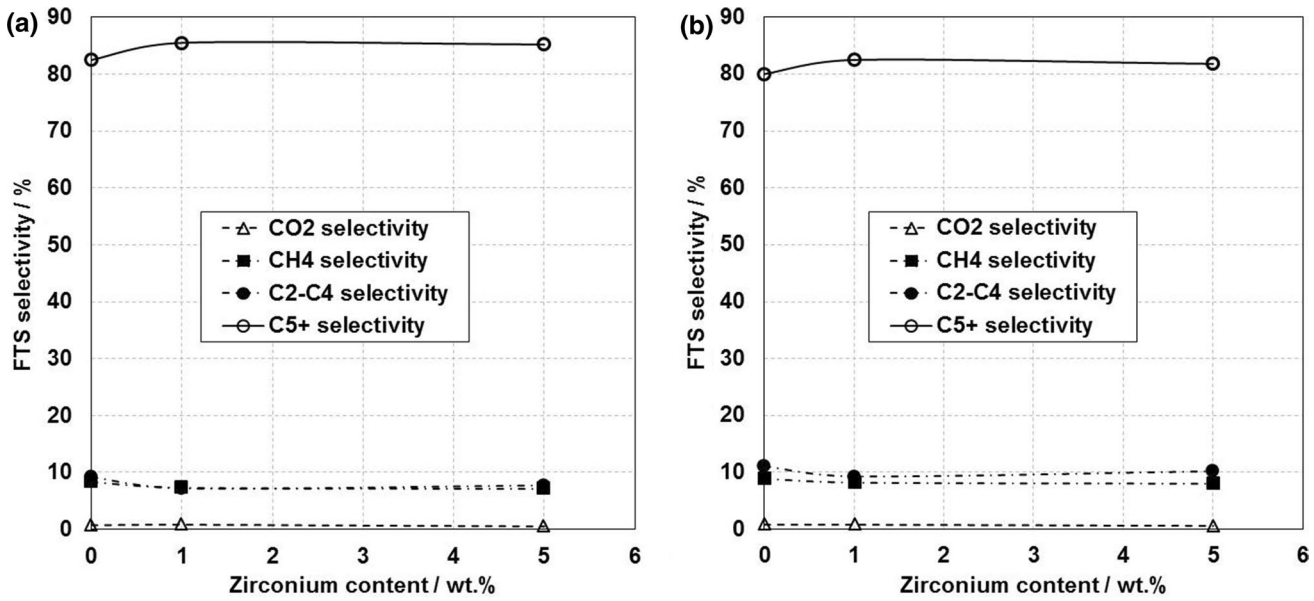

Fig. 2 Effect of Zr content in Co catalyst; CSTR reactor, 493 K, 2.2 MPa, 50% CO conversion, 25 wt% Co; H_2:CO = 2.1; TOS = 8–50 h (**a**), TOS = 50–120 h (**b**) Data from [26]

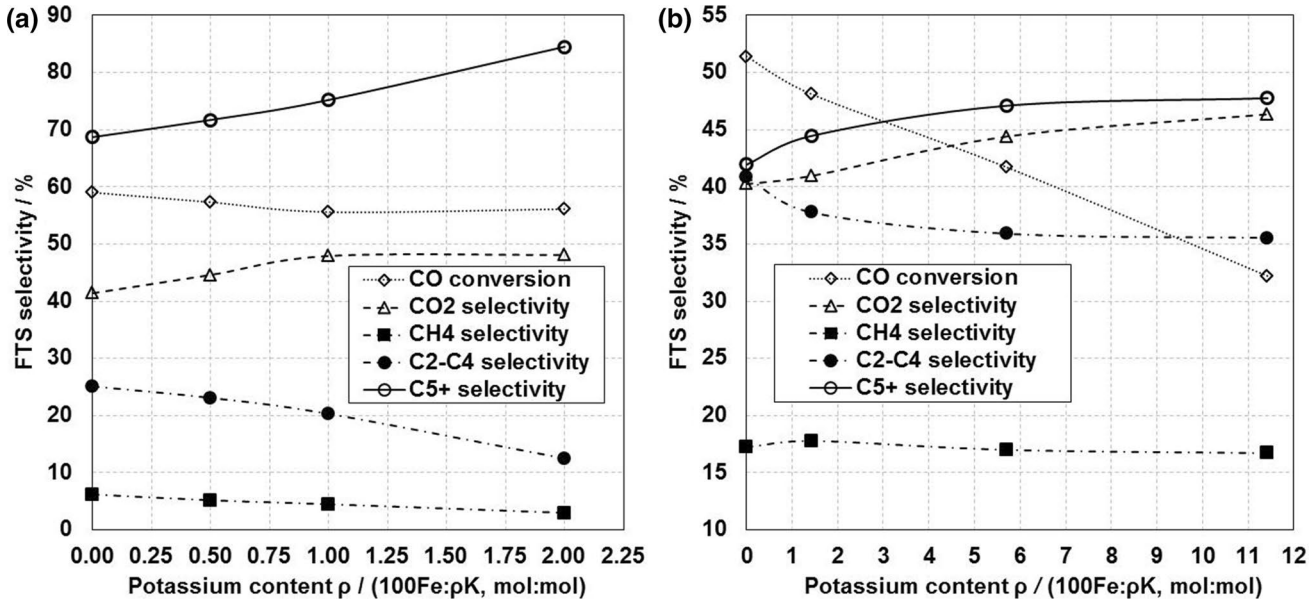

Fig. 3 Effect of potassium content on FTS; **a** CSTR, 543 K, 1.2 MPa, 3 $dm^3/g_{cat}/h$; H_2:CO = 0.7, carbon nanotubes catalyst support [41]; **b** fixed-bed reactor, 573 K, 1 MPa, 2.2 $dm^3/g_{cat}/h$, H_2:CO = 1.1; Fe content: 10 wt%, carbon coated silica catalyst support [39]

and CSTR slurry reactor as well (Fig. 3). The optimal K concentration for CSTR reactor was found as 0.5 mol% of iron loaded to the catalyst (Fig. 3a). Another increase of K results in gradual C_{5+} selectivity increase, nevertheless decreasing CO conversion and raising WGS activity result in low yields of organic liquid product. Deactivation rates of promoted and unpromoted catalysts reached near-identical values. The main deactivation route was formation and deposition of coke particles on active carbide phase. Authors highlight the need of K content optimization. Too low or zero K content during long-term run results in deactivation by reversible iron reoxidation of active carbide phase. Too high K content results in faster deactivation by coke formation and deposition. Experiments in reactor with fixed bed of catalyst (Fig. 3b) showed similar trends to those observed in CSTR reactor. Increase of K content up to almost 12 mol% of iron amount significantly reduces CO conversion. Depicted data show reaching maximal of selectivity to C_{5+} products over the catalyst with 5.7 mol% of K (related to Fe content). Trends of selectivity to other product were stabilized by increasing K content to this level.

Potassium promoter can be combined with sulfur in the role of another promoter. Similar to sulfur-free catalysts (Fig. 3b), the increase of potassium content evokes decrease in Co conversion, but results in higher selectivity to C_2–C_4 products and lower selectivity to C_{5+} products (Fig. 4a). Thus, presence of K in low concentrations increases selectivity of C_{5+} products and in concentrations higher than units of mol% of iron content evokes significant decrease of CO conversion. As shown in Fig. 4b, undesirable low conversion caused by high K content in catalyst can be changed by section of proper Fe:K:S ratio.

Doubling of content of both promoters in active phase with 30 wt% of iron results in little decrease of CO conversion and more than 20% increase of C_{5+} selectivity [52]. On the other hand, increase of S content with constant Fe and K content evokes increase of C_2–C_4 selectivity and important decrease in CO conversion.

Selection of alkali metal promoter depends on catalyst support used. Potassium is generally used in combination with SiO_2 derived supports, while in the case of SiC as catalyst support sodium is preferred. Similar to the effect of K, significant increase of Na in catalyst results in rapid decrease in CO conversion accompanied by increase of selectivity of C_{5+} products (Fig. 5a).

Fixed sodium content shows maximal CO conversion in trend of sulfur content increase (Fig. 5b) which is used as promotor as well. Maximal conversion was reached over catalysts with S content in the range 1.75–3.5 mol%. Higher content of sulfur in the catalyst results in rapid decrease in CO conversion. For using Na promoter together with S it is better to load these elements in the form of Na_2S than separately as Na_2O and elemental S. Sodium sulfide is better for promoters for its higher negative charge and more efficient bond configuration. Na_2S weakens hydrogen adsorption to carbon in Fe_5C_2 and strengthens hydrogen adsorption to reduced iron. This reduces methanation and increases selectivity to olefins [53].

The use of alkali metals as promoters can be summarized together with the role of sulfur the way, that iron catalyst are

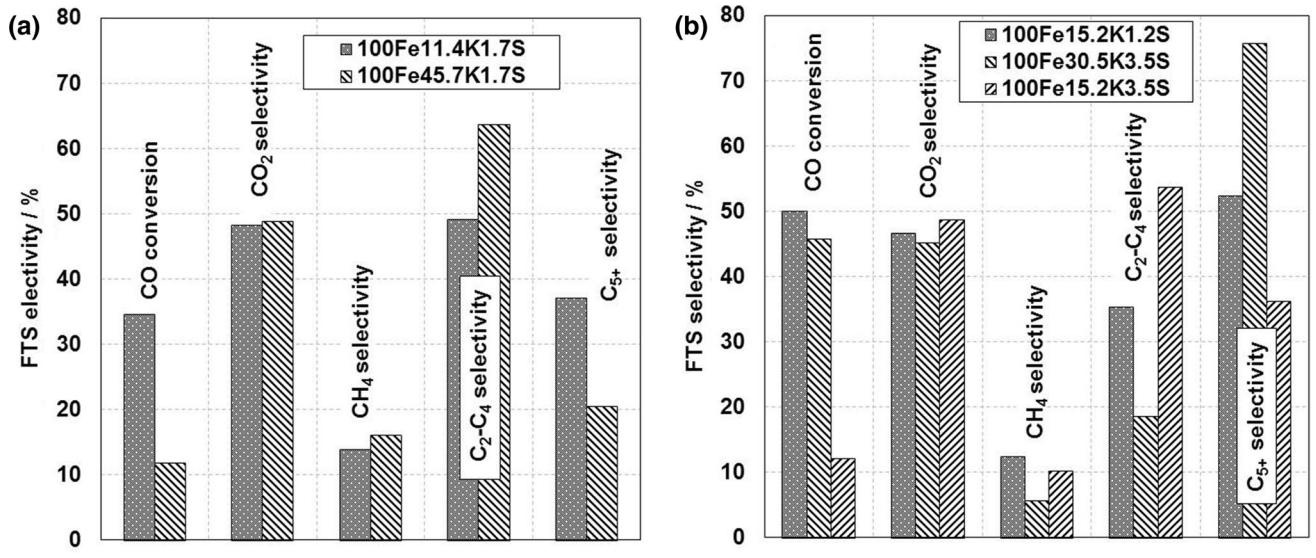

Fig. 4 Effect of K content in catalyst (**a** 10 wt% Fe; 573 K, 1 MPa, 2.2 $dm^3/g_{cat}/h$, H_2:CO = 1.1) and effect of different K:S ratios in catalyst (**b** 30 wt% Fe, identical reaction conditions), carbon coated silica catalyst support Data from [39]

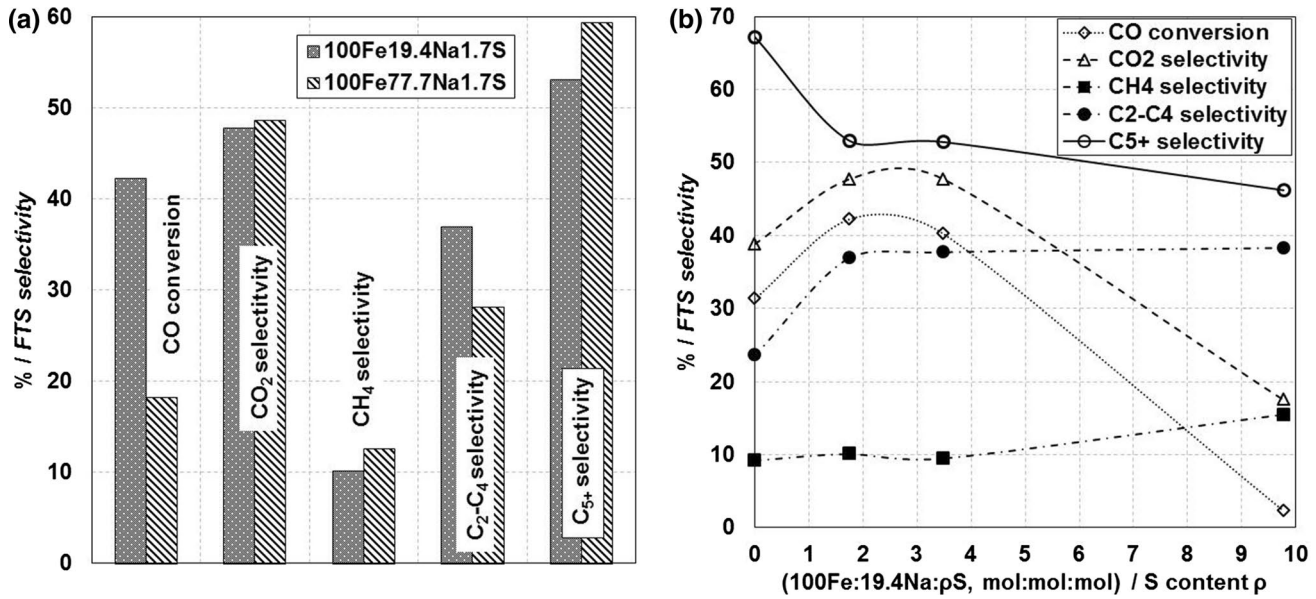

Fig. 5 Effect of sodium content (**a**) effect of sulfur content (**b**) on catalysts supported with SiC (**a**) and SiO_2 (**b**) 10 wt% iron, 573 K, 1 MPa, 2.2 $dm^3/g_{cat}/h$, H_2:CO = 1.1 Data from [39]

very sensitive to concentrations of these promoters, nevertheless the crucial is the combination of these promoters and their concentrations in active phase. Active phase of SiO_2 supported catalysts showed as optimal atomic ratio 100Fe:19.4Na:1.7S. Optimal composition of SiC supported catalysts was identified as 100Fe:19.4Na:1.75–3.5S [39]. In combination with α-Al_2O_3 the presence of Na and S causes increases selectivity of C_2–C_4 olefins, overall activity and lower methane selectivity (below 20% of carbon) [52]. Sodium reduces methanation and increases chain growth probability. Presence of sulfur is responsible for lowering of coverage of active phase particles with hydrogen.

Copper as another iron catalyst promoter simplifies reduction of iron without any effect on catalyst activity. Cu promotes reduction of Fe_2O_3 by providing centers for dissociation of adsorbed molecules of hydrogen. Content of iron carbides increases with raising content of copper in active phase. Concentration of carbides reaches maximal value in catalysts with Cu:Fe atomic ratio 0.02 [54]. During the activation, presence of copper evokes formation of

Fe-Cu clusters and suppresses initial iron carburization into active carbides. This results in lower FTS and WGS activity. Decrease of activity caused by copper results in significantly lower conversion (around 50% in comparison with copper free catalyst) as shown in Fig. 6. Copper content of 4.5 atomic% (related to iron) strongly reduces CO conversion and another increase to 11.2% does not affect conversion anymore. The main contribution of copper promoter use in iron catalysts is higher selectivity to C_{5+} products. This effect gets less significant at higher reaction temperatures (Fig. 6a vs. b). Increase of reaction temperature releases differences in selectivity caused by copper presence in active phase and lower conversion degree remains as the only significant change in catalyst activity.

Use of copper as promoter evokes changes in ratio of internal and α-olefins. Increase in formation of internal olefins over copper-containing catalysts is attributed to promotional effect of copper in hydrogen adsorption on catalyst surface related with higher hydrogenation and isomerization activity of catalyst. Analysis of aqueous phase pointed to higher content of dissolved oxygenates in products obtained from copper promoted iron catalysts caused by easier initiation of CO adsorption to the catalyst surface and followed with partial inhibition of its dissociation. As a result, the possibility of CO reaction with hydrogen and oxygen elimination is lower. Oxygenates formed are represented mainly by alcohols. Increase of copper content causes lower yields of methanol and ethanol balanced with significantly higher yields of C_{3-5} alcohols. The impact of copper content to iron catalyst is very similar to the use of potassium as a promoter. This was explained by catalysts' analysis using XANES/EXAFS method. Similar behavior of copper and potassium is given by formation of copper in oxidation state Cu^+ during standard activation procedure by syngas. Copper in this state has very similar properties to K^+ [56].

Together with copper, some other promoters can be used, such as MgO which stabilizes iron and avoids sintering. The final catalyst has then active phase formed of smaller crystallites with higher active surface area and higher catalytic activity than could be reached without use of MgO [54].

Manganese is attractive promoter for catalysts designed for production of light olefins. Presence of manganese evokes strong interaction Mn–Fe that results in higher catalytic activity. Increase of Mn content in catalyst results in suppressing formation and deposition of carbon deposits on active surface of the catalyst. Suppressing of carbon deposits formation is caused by lower concentration of Fe_xC carbides in active phase and higher value of CO hydrogenation activity in the presence of Mn. Manganese allows formation of $(Fe_{1-y}Mn_y)_3O_4$ phase which is responsible for the presence of smaller and more active Fe_xC particles with higher hydrogenation activity. Higher hydrotreating activity reduces sensitivity of catalysts to formation of carbon deposits [57]. Together with high reaction temperatures over 570 K, manganese evokes high content of C_2–C_4 olefins reaching 60% in organic phase of product [58]. In the case of hydrothermal loading of MnO_2 onto the hematite core, so called core–shell catalysts can be prepared. This catalyst type showed significantly accelerated CO dissociation on catalyst surface causing elevated intermediates on catalyst surface. These

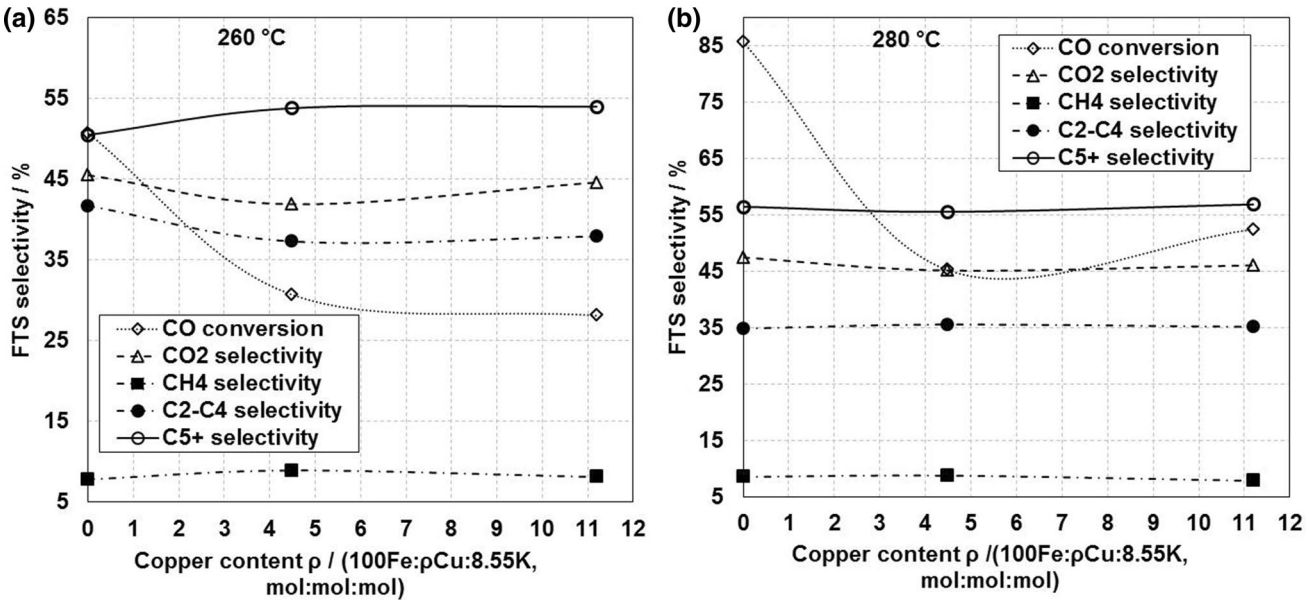

Fig. 6 Effect of copper content on FeK catalyst supported with active carbon at 533 K (**a**) and 553 K (**b**); 15.7 wt% Fe, 2.07 MPa, 3.0 $dm^3/g_{cat}/h$, H_2:CO = 0.9, fixed-bed reactor. Data from [55]

adsorbed intermediates are precursors of hydrocarbon chains formation; thus higher concentration of these intermediates results in higher C_{5+} selectivity and significantly lower selectivity to methane from 16 to 8.9% [59].

Nickel and zirconium are other potential promoters of iron catalysts. Zr strongly inhibits reduction and carburization of iron particles of active phase by very strong Fe–Zr interaction resulting in lower catalytic activity (Fig. 7). Nickel addition to the catalyst increases activity and reduces C_{5+} product selectivity. As another effect, presence of Ni evoked higher WGS activity.

Catalyst supports

Ruthenium and cobalt catalysts are usually supported catalysts with active metal content in the range of units of wt% (Ru) or up to 30 wt% (Co). Lower content of Ru is given by combination of high activity, requirement of high Ru dispersion, and high prices of Ru. High cobalt loading is used in aiming to maximize cobalt phase surface, which is the rate-determining parameter. Another reason of catalytic supports' use is electron interaction of active phase and support material with significant impact to catalyst activity (FTS, WGS) and product selectivity. Interaction of active phase with support material is typically accompanied by formation of mixed phases.

Cobalt catalysts are currently the most intensively studied type and exclusively preferred for industrial applications. These catalysts can be combined with wide scale of supports, typically oxides with different load of active metal. One of the most common materials is alumina. Especially γ-Al_2O_3 followed by some other crystalline modifications are

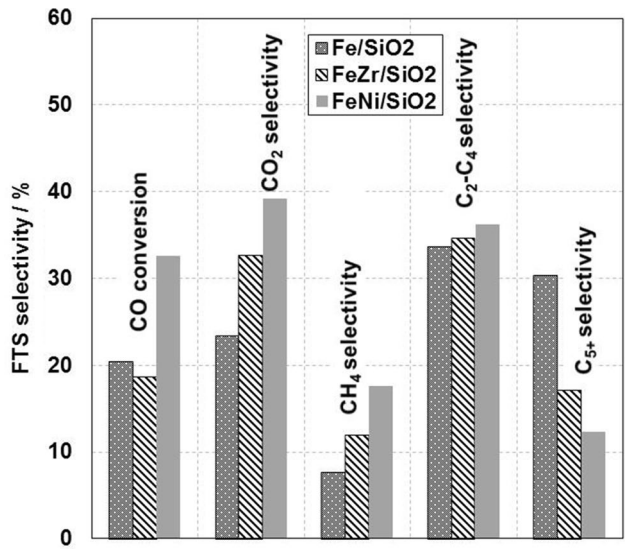

Fig. 7 Effect of Zr and Ni on FTS; fixed-bed reactor, 523 K, 0.1 MPa, GHSV = 1 $dm^3/g_{cat}/h$, H_2:CO = 0.69. Data from [40]

frequently used in FTS studies [11, 13, 15, 17, 23, 24, 26, 27, 46, 60–72]. Disadvantage of γ-Al_2O_3 support is sensitivity to liquid water and vapor (high water partial pressure) in reaction mixture at reaction temperatures around 493 K and higher. Presence of water and its vapor at elevated temperatures evokes changes in catalyst supports crystallinity and catalytic properties of the catalyst.

Comparison of Co_3O_4 activity in unsupported form in mesoporous (formed by loading to KIT-6 and leaching in NaOH) and compact form [60] showed significantly lower activity of compact material due to very low specific surface area (32 m^2/g). CO conversion over the compact active phase reached only 6.1% despite to almost complete reducibility at temperatures up to 723 K. Mesoporous Co_3O_4 was less reducible and had three times higher specific surface area and provided double CO conversion than compact one. Both active phases were found as stable with constant CO conversion in the first 20 h of catalytic experiment. Stable conversion decrease can be explained by very low conversion degree. Insertion of aluminum into mesoporous Co_3O_4 (impregnation with $Al(NO_3)_3$) evokes significant increase in CO conversion from 12 to 88% after 20 h on stream. The conversion decreased to 84% between 20 and 40 h on stream at 503 K. Combining Co and Al components (Co:Al = 1:0.125; mol:mol) by coimpregnation to KIT-6 (SiO_2 removed with leaching in NaOH) results in 94% CO conversion at 513 K between 20 and 40 h on stream. Doubled Al content increases further conversion decrease to 96%, but faster deactivation as well. The effect of Al (Al_2O_3 respectively) in Co_3O_4 phase can be concluded as enabling of $CoAl_2O_4$ spinel phase and increasing of mesopores' stability. The presence of aluminum in such low concentrations stabilizes porous structures of Co_3O_4 by strong interaction with internal surfaces of the catalyst and with of Co_3O_4 and Al_2O_3 interaction in mixed oxides of the main framework of the catalyst. However, these catalysts are not the classic supported catalyst.

In supported catalysts, the support material usually represents the main component of the catalyst matter. Thus it is necessary to take into account the catalyst stability from the point of view of the active phase and support with the same importance. Difference in stability is very significant by comparison of mesoporous Al_2O_3 and γ-Al_2O_3 [17]. Mesoporous material with higher specific surface area is more exposed to the reaction mixture than in the case of conventional γ-Al_2O_3 supported catalyst with identical cobalt load and half value of specific surface area and pore volume. Despite identical method of cobalt loading to the support, mesoporous catalyst reached lower CO conversion between 100 and 120 h on stream (Fig. 8a).

Authors described that catalyst with mesoporous support can reach higher activity than γ-Al_2O_3 in the case of loading cobalt precursor in acetone and ethanol solutions instead of

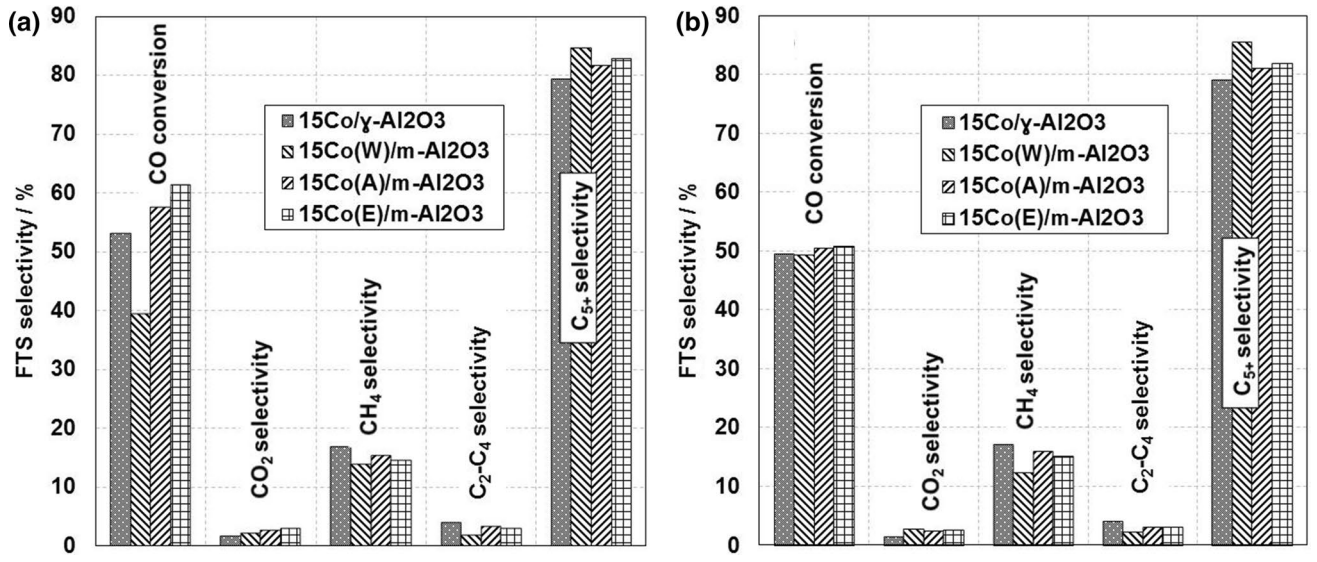

Fig. 8 FTS products quality over catalysts prepared with different solutions for Co precursor loading on mesoporous (m) support in comparison with Co/γ-Al_2O_3. Fixed-bed reactor, 503 K, 2.07 MPa; *E* ethanol, *A* acetone, *W* water; **a** GHSV = 0.9 $dm^3/g_{cat}/h$, **b** GHSV changed to reach 50% CO conversion. Data from [17]

aqueous solution. The change of solvent in Co precursor solution helps to reach higher selectivity to C_{5+} products as well (Fig. 8a). The comparison of catalyst at similar (50%) CO conversion shows little differences in selectivity of formation of C_2–C_4 and C_{5+} products (Fig. 8b), which were little higher than in products obtained over γ-Al_2O_3 supported catalyst. From the activity point of view, loading of Co precursor in ethanol solution was found as the most efficient.

The role of Co content in the mesoporous alumina supported catalyst results in increasing CO conversion with raising Co content from 15 to 30 wt%. Product selectivity is not sensitive at identical reaction conditions (Fig. 9a); nevertheless at similar conversion degree, the higher Co content results in lower CO_2 and CH_4 selectivity and higher C_{5+} selectivity (Fig. 9b).

Alumina is usually used for catalysis with γ-crystalline structure. This material is usually produced thermally from precursors, which are typically boehmite or gibbsite. Different thermal treating is the way to prepare various Al_2O_3 crystalline structures with different properties. Thermal

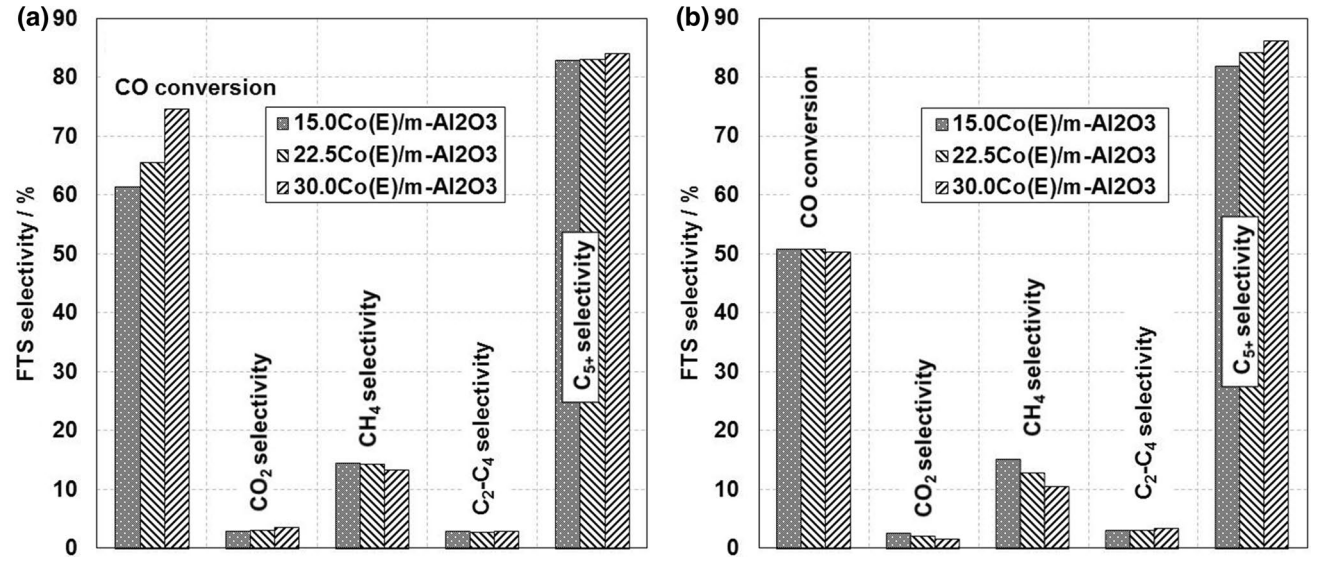

Fig. 9 FTS products quality based on Co content in mesoporous alumina supported catalysts. Fixed-bed reactor, 503 K, 2.07 MPa; *E* ethanol, **a** GHSV = 0.9 $dm^3/g_{cat}/h$, **b** GHSV changed to reach 50% CO conversion. Data from [17]

treating of boehmite at different temperatures and different time of exposure is the way for synthesis of γ, δ, and θ crystalline structured Al_2O_3. *X* and κ Al_2O_3 can be prepared from Gibbsite. Thermal treating does not affect just crystalline structure. Porous parameters vary depending on heat of calcination. The specific surface area decreases with raising heat of calcination in case of both precursors (Fig. 10a), while pore volume is not affected that much for calcination of boehmite and in the case of gibbsite treating remains almost constant (Fig. 10b). Experiments with catalysts with 20 wt% of cobalt loaded to supports prepared by thermal treating pointed to boehmite as optimal Al_2O_3 precursor, when calcined at 1000 K for 10 h. Catalyst support prepared this way has specific surface area, 84 m^2/g, which is lower than after 3 h of calcination. This support allows reaching higher selectivity to C_{5+} products and lower selectivity to CO_2 and CH_4 in comparison with other catalysts [15].

Porosity and mean pore volume of γ-Al_2O_3 catalyst support play an important role in catalyst activity and stability of cobalt active phase [26]. Comparison of catalysts prepared using commercially available wide-pore Al_2O_3 (Puralox HP14150 wide-pore Al_2O_3, mean pore diameter 25 nm) with narrow-pore (Catalox150 narrow pore Al_2O_3; mean pore diameter 10.8 nm) shows significantly higher activity of catalyst with wide-pore support, that was about 40% higher than activity of narrow-pore supported catalyst. Moreover, the wide-pore Al_2O_3-supported catalyst is more stable and resistant to deactivation and has higher selectivity to C_{5+} products and lower selectivity to CH_4 [26].

The catalyst stability is very important for catalyst lifecycle and process economy. TiO_2, SiO_2 and their combinations with other oxides are investigated to optimize catalyst stability and selectivity to required products. Catalysts with these supports can reach the same or better catalytic parameters then conventional Al_2O_3-supported catalysts.

Comparison of 15 wt% Co catalysts supported with γ-Al_2O_3 and SiO_2 (Fig. 11) shows similar overall catalyst activity of both catalysts despite the smaller Co particles size of Co/γ-Al_2O_3 and little higher pressure (2.76 MPa) in testing this catalyst. Co/SiO_2 catalyst in this comparison has higher selectivity to CO_2 and C_{2+} products' formation and lower selectivity to CH_4.

Porosity of catalyst supports can significantly affect diffusion of reactants in catalyst particles. As shown before (Figs. 8 and 9), catalysts with this type of porosity can provide the same or higher catalytic activity as conventional catalyst supports. In the case of SiO_2-based supports, mesoporous cellular foams (MCF) of different mesoporous silicas were reported as potential catalyst supports for Co catalysts (Fig. 12) [73].

This comparison shows lower selectivity to undesirable CH_4 and less attractive C_2–C_4 products and higher selectivity to C_{5+} products over MCF supported catalysts than over mesoporous supported catalysts. CO conversion over SBA-15 supported catalyst is approximately half in comparison with other catalyst without any significant change in product selectivity. SBA-15 supported catalyst shows the lowest selectivity to C_{5+} products. FTS product is CO_2 free for all the catalysts used. Based on depicted results, optimal pore

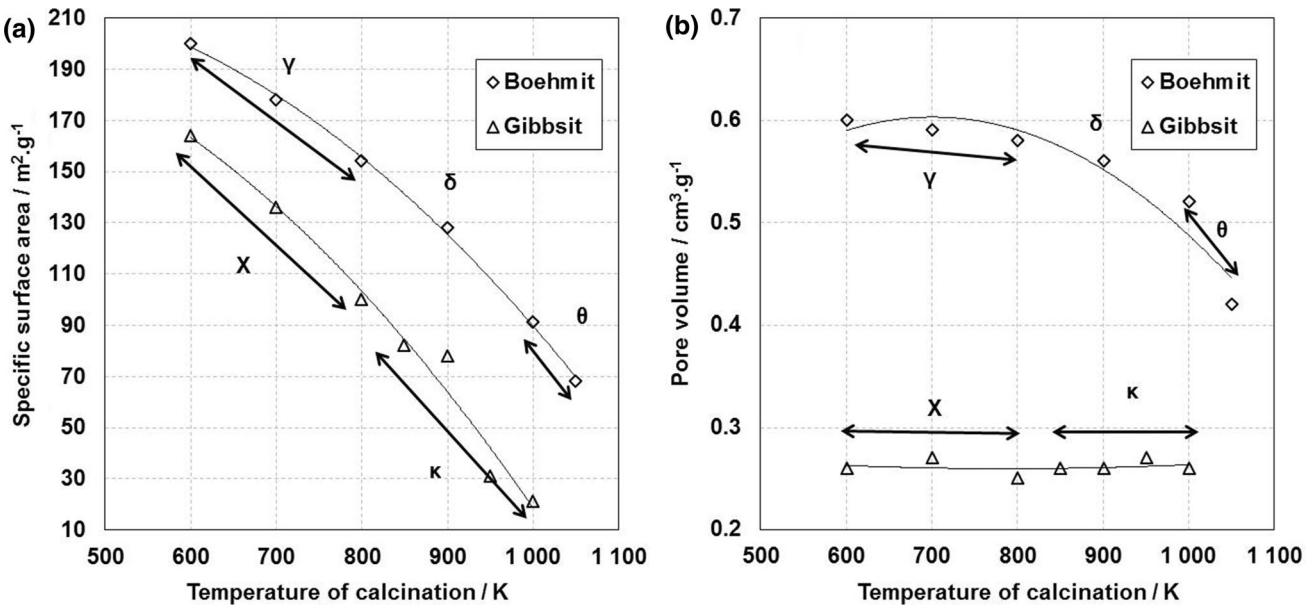

Fig. 10 Effect of temperature calcination on crystalline structure and specific surface area (**a**) and pore volume (**b**). Materials calcined for 3 h. Data from [15]

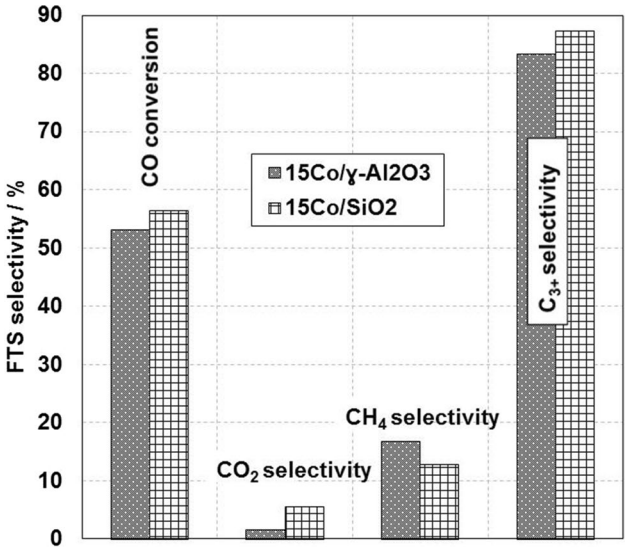

Fig. 11 Comparison of Al_2O_3 [17] and SiO_2 [29] as supports for 15 wt% Co FTS catalysts, 503 K, 2.76 MPa (Al_2O_3), 2.0 MPa (SiO_2), H_2:CO = 2, GHSV = 0.9 $dm^3/g_{cat}/h$; Al_2O_3: catalyst as "dust" (less active of the set), SiO_2 particle size 0.5–1.0 mm

size for maximal conversion is 8.8 nm, while the optimal for maximal C_{5+} selectivity is support with 16.3 nm (Fig. 13a).

The role of Co crystallites size is depicted in Fig. 13b. Catalysts were prepared using MCF with pore size 18 nm. Particle size of Co crystallites was controlled by defined addition of citric acid during impregnation of Co on catalyst support. Results show positive effect of crystallites' size increase in raising Co conversion and selectivity to C_{5+} products. Trend of CO conversion shows potential maximal conversion for catalysts with Co particle size around 9 nm. Crystallite size can be expressed as an equivalent of active surface defining adsorbed amount of reaction intermediates and precursors of C_yH_x species' oligomerization. These intermediates and precursors can interact and form larger compounds at the surface of one crystallite. Thus, larger crystallite statistically allows formation of larger hydrocarbon molecules than smaller crystallites. Optimal crystallite size affects catalytic activity and FTS selectivity, but it is necessary to take into account that optimal crystallite size is always influenced by reaction conditions which affect equilibrium of reactions on active sites. The most important reactions are dissociative adsorption of CO and H_2. Based on this, syngas conversion and reaction selectivity (and optimal crystallites size, respectively) depend strongly on syngas space velocity (gas hourly space velocity, GHSV).

Zeolites were studied in the role of cobalt catalyst supports as well, for example ZSM-5 and its mesoporous modifications. Results showed little higher CO conversion over catalysts with mesoporous ZSM-5 as well as rising conversion with increasing mesopore volume (Fig. 14a). Change from microporous to mesoporous ZSM-5 results in significantly different product distribution. Mesoporous nature of the catalyst significantly increased selectivity to C_{5+} products and significantly reduced selectivity to CH_4. The use of mesoporous support negatively affects CO_2 selectivity which rose from zero to units of %. Compared to SBA-15 supported catalysts, microporous and mesoporous ZSM-5-based materials are less active (Fig. 14b) with significantly lower selectivity to C_{5+} products and higher production of undesirable methane. On the other hand, Co/SBA-15 is less stable with significantly higher deactivation rate between 24 and 240 h on stream. The lowest deactivation rate was described for Co/MZ1 with mesopore volume 0.24 cm^3/g (Co/MZ2: 0.38 cm^3/g; Co/MZ: 0.65 cm^3/g; Co/ZSM-5: 0 cm^3/g). The deactivation rate rose with increasing mesopore volume [74].

Kang and co-workers described the effect of mesoporous structure in combination with method of cobalt loading to zeolites Y [33]. Authors described that catalysts prepared by classic incipient wetness impregnation, especially mesoporous catalysts reach ca 5% lower CO conversion.

Similarly, catalysts with melt-impregnated active phase were less selective to C_{5+} products. As described

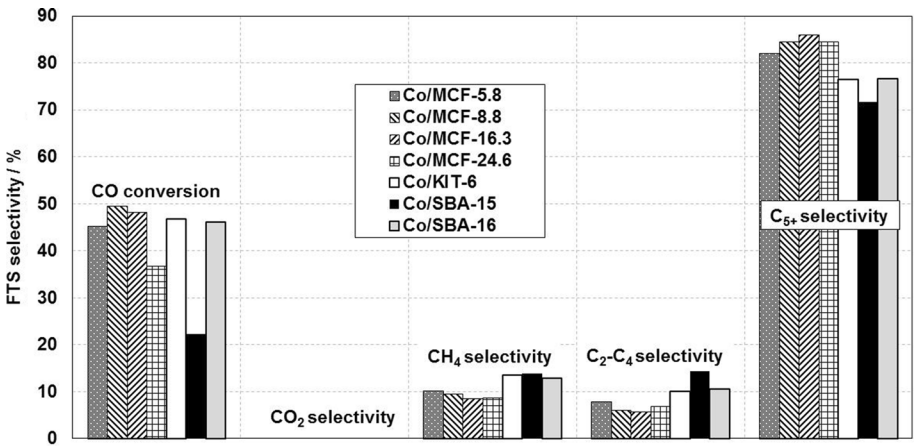

Fig. 12 Comparison of FTS products over 15 wt% catalysts supported with different SiO_2 supported catalysts; fixed-bed microreactor, 483 K, 1.0 MPa, H_2:CO = 2, GHSV = 4 $dm^3/g_{cat}/h$. Number behind "MCF" refers to mean pore diameter (nm) of catalyst support. Data from [73]

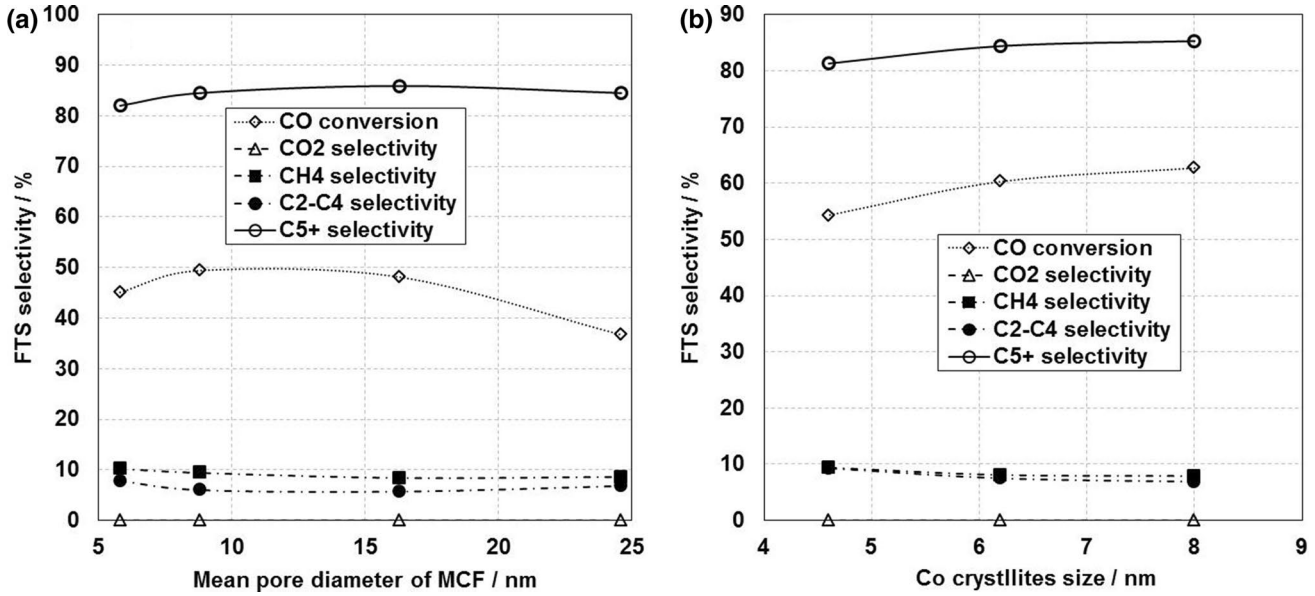

Fig. 13 Effect of mean pore size diameter (**a**) on FTS selectivity and effect of Co crystallite size (**b**), mean pore diameter 18 nm (15 wt% of Co), fixed-bed microreactor, 483 K, 1.0 MPa, H_2:CO = 2, GHSV = 4 $dm^3/g_{cat}/h$, TOS = 24 h. Data from [73]

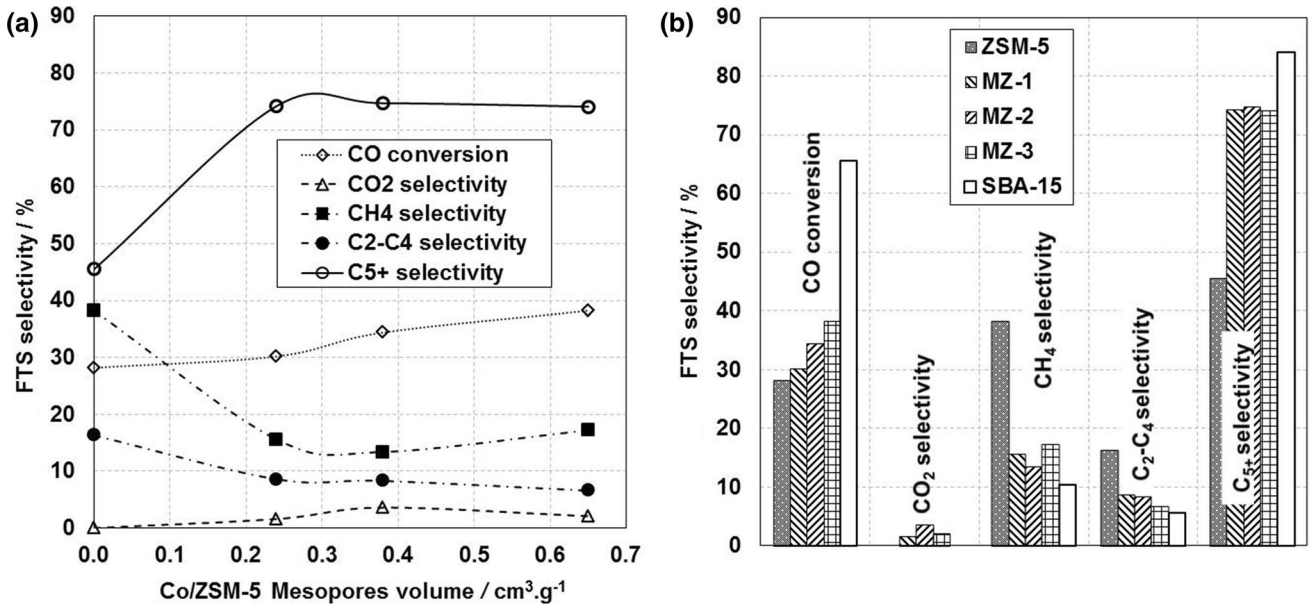

Fig. 14 Effect of mesopores volume of Co/ZSM-5 (**a**) and activity comparison for cobalt catalysts with ZSM-5, meso ZSM-5, and SBA-15 as supports (**b**). 15 wt% of Co, fixed-bed reactor, 493 K, 2 MPa, H_2:CO = 2, GHSV = 1.2 $dm^3/g_{cat}/h$, TOS = 24 h. Data from [74]

for ZSM-5 catalysts (Fig. 14), the presence of mesopores brings important increase of C_{5+} and reduced CH_4 and C_2–C_4 selectivity for Y-zeolite based catalysts as well (Fig. 15a). In combination with melt impregnation, the increase of mean pore diameter results in little higher CO conversion, while for impregnated Co active phase presence of mesopores evokes little decrease in conversion (Fig. 15b).

Another potential support for cobalt catalysts are SiC and TiO_2. Comparison by Zhu and coworkers [29] shows that TiO_2 supported catalyst is significantly more active than SiC supported catalyst at 478 K (Fig. 16a). The same Co/SiC catalyst was found as more active at 503 K with higher

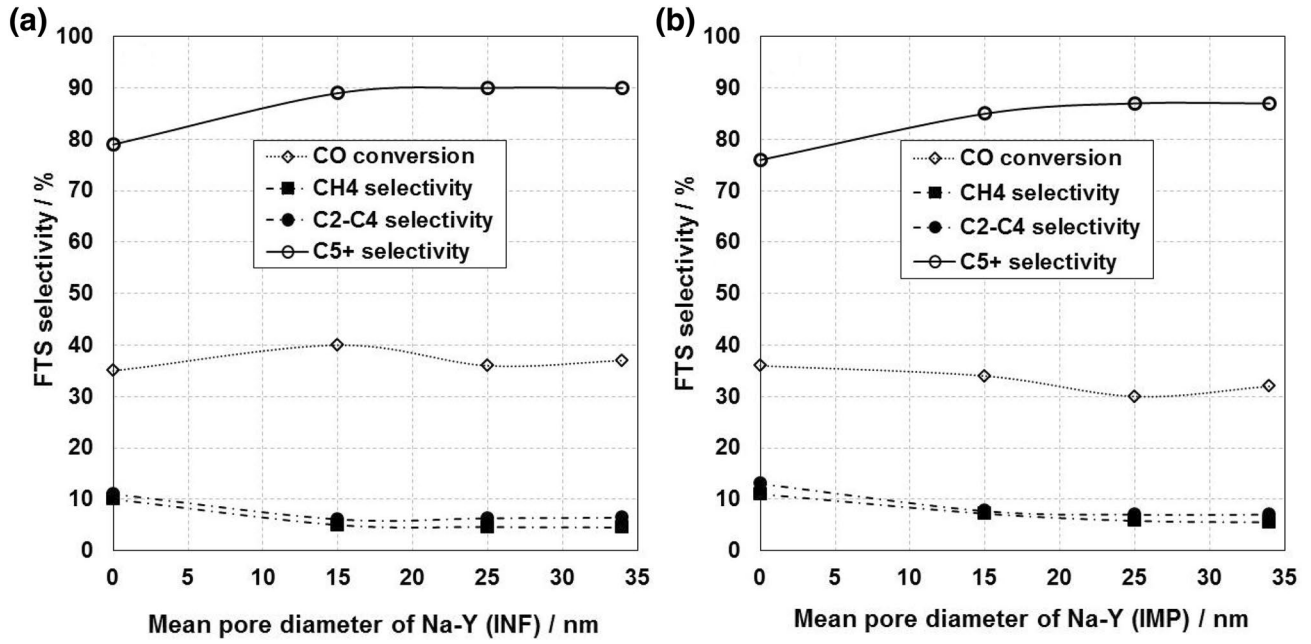

Fig. 15 Effect of mean pore diameter of Na-Y of catalysts prepared by melt infiltration (**a**) and by classic impregnation with cobalt nitrate hexahydrate (**b**), 1 wt% of Co, fixed-bed reactor, 503 K, 2.0 MPa, H_2:CO = 1, GHSV = 2.4 $dm^3/g_{cat}/h$. Data from [33]

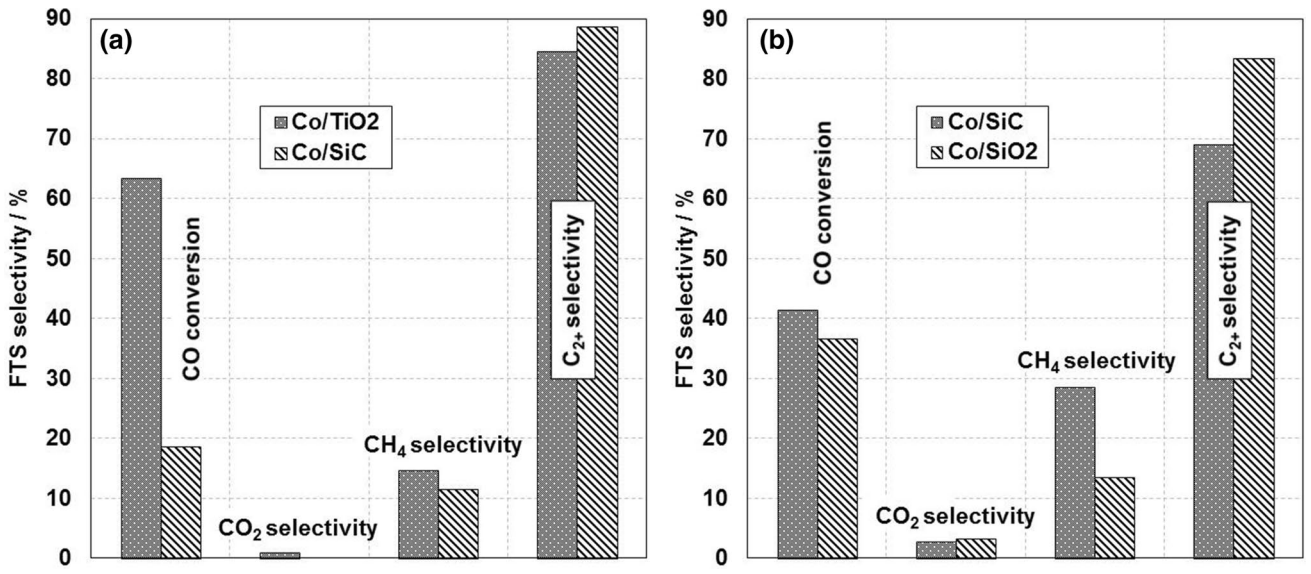

Fig. 16 Comparison of TiO_2 and SiC as supports of Co catalysts (15 wt%) at 478 K (**a**) and comparison of SiC and SiO_2 at 503 K, 2 MPa, GHSV = 1.35 $dm^3/g_{cat}/h$; fixed-bed reactor. Data from [29]

conversion and C_{5+} selectivity than Co/SiO_2 (Fig. 16b). Based on the description, TiO_2 is more selective to C_{2+} products formation, which in the case of SiC decreased after increasing of reaction temperature from 478 to 503 K. At this reaction temperature, Co/SiO_2 is more selective to C_{2+} product formation than Co/SiC one.

When selecting TiO_2 as catalyst support for low-temperature FTS catalyst, it is recommended to use rutile crystalline phase, which allows reaching higher CO conversion and selectivity to liquid C_{5+} products than with-anatas supported catalyst [21]. For Ru-promoted Co/anatas catalyst, some changes in catalytic activity were described in dependence of metal-support interaction, which significantly changes with the value of specific surface area of anatas. For these catalysts the relative activity decreases with increasing specific surface area of the support

material and thus with increasing intensity of cobalt–anatas interaction [75].

The alternative to oxide catalyst supports are catalysts on carbon basis, such as active carbon or carbon nanofibers (CNF). These supports have specific lower electron interaction with cobalt than in oxide supports. This is the cause of problematic binding of cobalt to the surface of catalyst support. Cobalt is weakly fixed to the support and this weak interaction results into high probability of active phase releasing during reaction. Another risk of weak interaction is in increased probability of cobalt particles sintering or by formation of too large active particles by Ostwald ripening. Carbon-based catalyst support thus requires pretreating before cobalt precursor loading. These modifications serve to roughen the support surface for reducing mobility of cobalt particles on the support surface. One of the methods for pretreating the surface is treating of CNF in concentrated nitric acid under defined conditions creating rough surface with barriers that separate cobalt crystallite at the support surface. This layout of crystallites significantly slows down cobalt sintering and stabilizes binding of active phase to the support during the reaction.

High-temperature iron catalysts are studied with and without catalyst supports. The comparison of unsupported catalyst with supported versions (both without any promoters) points to TiO_2 supported version to be only more active than unsupported catalyst at identical reaction conditions (Fig. 17a). Active carbon (AC) supported catalyst shows similar conversion as reference unsupported catalyst. This catalyst is the most selective to C_{5+} products. Comparison of AC with SiC as support points to significantly lower conversion over the Fe/SiC and the highest selectivity to C_2–C_4 products of all the catalysts compared. Fe/SiO_2 is less active than Fe/SiC. The advantage of SiO_2 support is the lowest selectivity to CO_2, but the selectivity to undesirable CH_4 is the highest in this comparison. The less active Al_2O_3 supported catalyst is attractive for high selectivity to C_{5+} products.

When using syngas with higher H_2:CO ratios than typically used for iron catalysts, significant changes can be observed in catalyst support comparison. Higher hydrogen partial pressure at the same reaction temperature allows reaching the same CO conversion under almost four times higher GHSV as during CO rich syngas reaction. CNF supported catalyst was found as the most active (Fig. 17b). Higher partial pressure positively affects reactivity over the Al_2O_3 supported catalyst, which is more active than SiO_2 supported one and has the highest selectivity to C_{5+} products. Mesoporous carbon as catalyst support (CMK-3) has the highest selectivity to C_2–C_4 products, but lower conversion than Al_2O_3 supported catalyst. The less active catalyst in this comparison is Fe/SiO_2.

The role of reaction conditions

Reaction conditions, such as reaction temperature and pressure, GHSV, and H_2:CO ratios in syngas strongly affect the conversion of syngas during FTS and product distribution. Selection of reaction conditions and catalyst type depends on qualitative parameters of products, for example alcohols, C_2–C_4 olefinic fraction, naphtha and diesel fraction or C_{25+} waxy compounds. Important role plays the syngas quality available (H_2:CO), however this can be modified before reaction by WGS to increase hydrogen content.

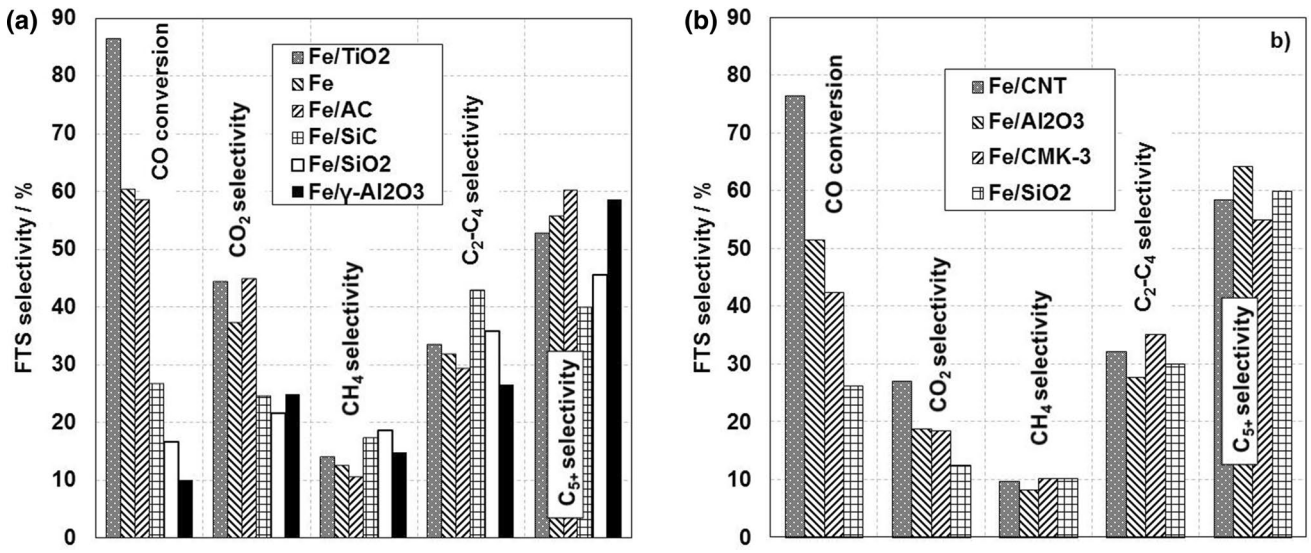

Fig. 17 Effect of catalyst support on CO conversion and reaction selectivity. 10 wt% Fe; fixed-bed reactor, 573 K; **a** H_2:CO = 1.1; 1 MPa, GHSV = 4.4 $dm^3/g_{cat}/h$ [39]; **b** H_2:CO = 2, 2 MPa, GHSV = 16 $dm^3/g_{cat}/h$ [76]

One of the most important reaction parameters is the reaction temperature. FTS is very sensitive to changes of this parameter which strongly affects syngas conversion and catalyst deactivation. Reaction temperatures around 513–523 K is the limit for catalyst use. Lower temperatures are typical for so-called low-temperature FTS catalyzed by cobalt and ruthenium catalyst, while higher temperatures are common for high-temperature FTS catalyzed by iron catalysts. Other important parameters are flow of syngas per amount of catalyst (GHSV), syngas composition, and reaction pressure.

The reaction pressure is important parameter of the reaction affecting the catalyst activity and distribution of hydrocarbon products. In general, an increase of hydrogen pressure results in higher catalyst activity and syngas conversion, respectively. Typically, the reaction pressure during FTS is adjusted to 2–3 MPa. Physical aspects, such as need of keeping the water produced by reaction in gaseous state to avoid catalyst deactivation, technically limit higher reaction pressure. The selection of reaction pressure has to be optimized based on some other aspects, for example catalyst activity, product parameters, and reactor type. Although it is possible to maximize reaction pressure to very high pressures and to maximize activity, condensation of water would result in faster catalyst deactivation. Higher reaction temperatures could avoid water condensation, but the change of hydrocarbon distribution to higher yields of light products is not usually required. The third disadvantage of high reaction pressure is important, especially for trickle and fixed bed reactors. These are known for limitations in heat transfer through the reactor wall. High increase of catalytic activity by increased pressure would result in rapid temperature increase along the reactor. To avoid uncontrolled reaction, an increase of GHSV is necessary to reduce overall conversion and to use excess of syngas as internal coolant. Another solution is expanding the relative heat exchange. The easiest way to promote heat removal is to reduce reactor (and catalyst bed) diameter together with reduction of catalysts' particle size. Although it sounds simple, reduction of reactor diameter and catalyst particles increases difficulty of reactor maintenance in the form of spent catalyst removal and loading the fresh one. Thus, increasing reaction pressure might be solution for temporary recovering of catalyst deactivation, but for reactor designing it brings many complications to be solved.

Cobalt catalysts

Cobalt active phase is highly sensitive to reaction condition changes and this makes this parameter to be one of the most important for syngas conversion and process selectivity. Comparison of CO conversion at different reaction temperatures shows significant raising conversion with increasing reaction temperature (Fig. 18a, [29]). Co/TiO_2 shows the highest sensitivity to changes of reaction temperatures with around 50% conversion increase after reaction temperature change from 468 to 478 K. Catalysts like this are appropriate for reactors with efficient reaction temperature controlling system. Co/SiC is not as sensitive to reaction temperature changes as previous one and is able to reach the same conversion degrees in wider temperature range 468–513 K. The

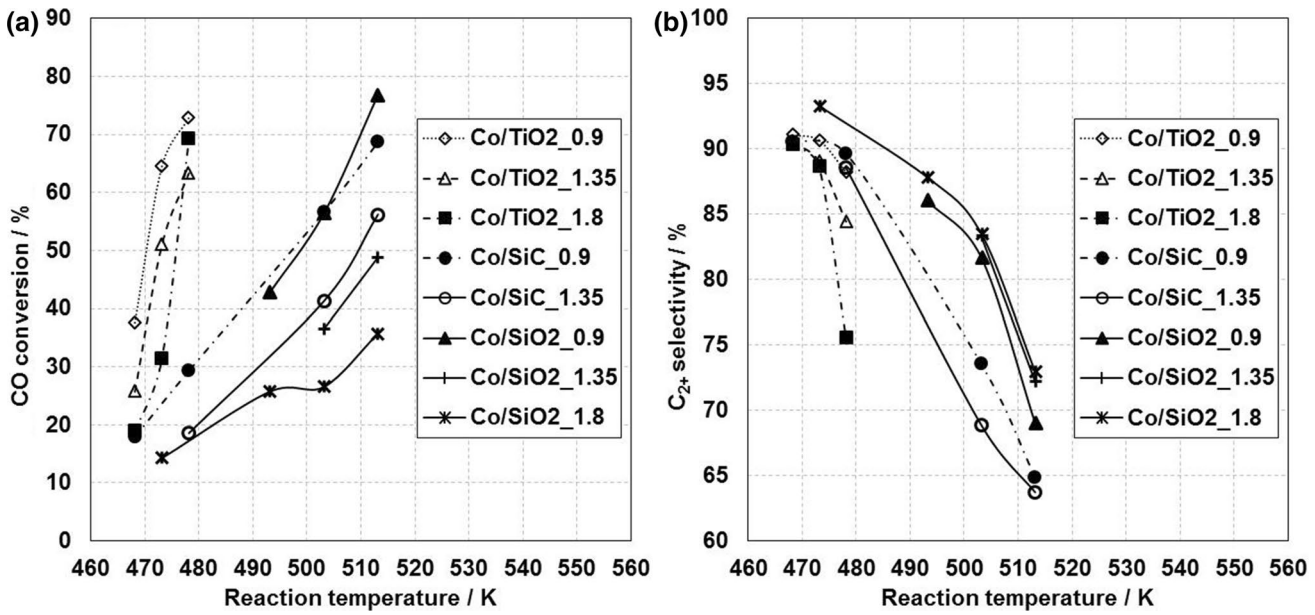

Fig. 18 Effect of reaction temperature on CO conversion (**a**) and selectivity to C_{2+} products (**b**). Fixed-bed reactor, 2 MPa, number in the end of catalyst mark refers to GHSV value ($dm^3/g_{cat}/h$), 15 wt% Co. Data from [29]

least sensitive is Co/SiO_2 with maximal CO conversion 77% at 513 K and low GHSV. The effect of reaction temperature is crucial for product distribution (Fig. 18b) showing significant decrease of selectivity to C_{2+} products' formation with increasing reaction temperature. The order of sensitivity of C_{2+} selectivity decreases in the following order: $Co/TiO_2 > Co/SiC > Co/SiO_2$.

Trends of long-term activity and product distribution over the Co/SiO_2 at low temperatures between 100 and 150 h on stream confirm trends of CO conversion and C_{2+} selectivity (Fig. 19a, [16]). CO conversion increases almost linearly in temperature range 458–483 K. At higher reaction temperatures and higher GHSV it is possible to reach similar product distribution at temperature up to 523 K with the $CoMn/SiO_2$ catalyst (Fig. 19b, [35]).

Conversion increase with increasing reaction temperature is significant also for Al_2O_3 supported catalysts with different modifications and promoters in other than fixed bed reactors. For example, trends of Co-Re catalyst in fixed bed reactor (Fig. 20a) and Co–Pt in microchannel reactor (Fig. 20b) are shown.

In CSTR reactor with suspended Co/Al_2O_3 catalyst the significant CO conversion increase takes place at reaction temperatures over 503 K (Fig. 21a). This conversion increase is related with rapid loss of selectivity to C_{5+} products. Co/ZrO_2 is at similar conditions less sensitive to changes of reaction temperature and more selective to C_{5+} products than Co/Al_2O_3 (Fig. 21b).

Similarly as reaction temperature, GHSV change significantly affects CO conversion and product selectivity. Generally, the increase of GHSV results in lower CO conversion (Fig. 22a) and little reduces selectivity to heavier products in case of cobalt supported with TiO_2 or SiC. In the case of Co/SiO_2, the selectivity to C_{5+} products increases at higher GHSV values (Fig. 22b).

Co/Al_2O_3 catalyst has similar tendencies of lower CO conversion and selectivity to C_{5+} products with increasing GHSV (Fig. 23a) as observed for Co/TiO_2 and Co/SiC catalysts. The decrease of production over the Co/Al_2O_3 can be compensated by increase of active metal content from 15 wt% to 25 wt%. Higher cobalt content reduces production of CH_4 and C_2–C_4 products that are undesirable products for fuel applications of FTS (Fig. 23b).

Syngas composition strongly affects FTS reaction. Presence of impurities can cause higher rate of deactivation, but catalyst inhibitors are supposed to be removed in syngas pre-treating stages before catalytic sections. From selectivity and activity point of view, H_2:CO plays an important role in catalytic activity. The role of this parameter can be easily described in the following way: CO conversion decreases with H_2:CO ratio decrease below 2. The CO conversion is the most sensitive to H_2:CO ratio increase from 1 to 2 (Fig. 24). Higher hydrogen partial pressure allows to increase CO conversion 4 times from 13 to 56% by H_2:CO ratio change from 1 to 2. Another increase of H_2:CO ratio does not increase CO conversion so strongly; nevertheless it strongly affects product distribution resulting in higher selectivity to methane and drop in selectivity to C_{5+} products.

The effect of reaction pressure on product composition is not as strong as in the case of changes in reaction temperature, GHSV, or syngas composition. In case of cobalt

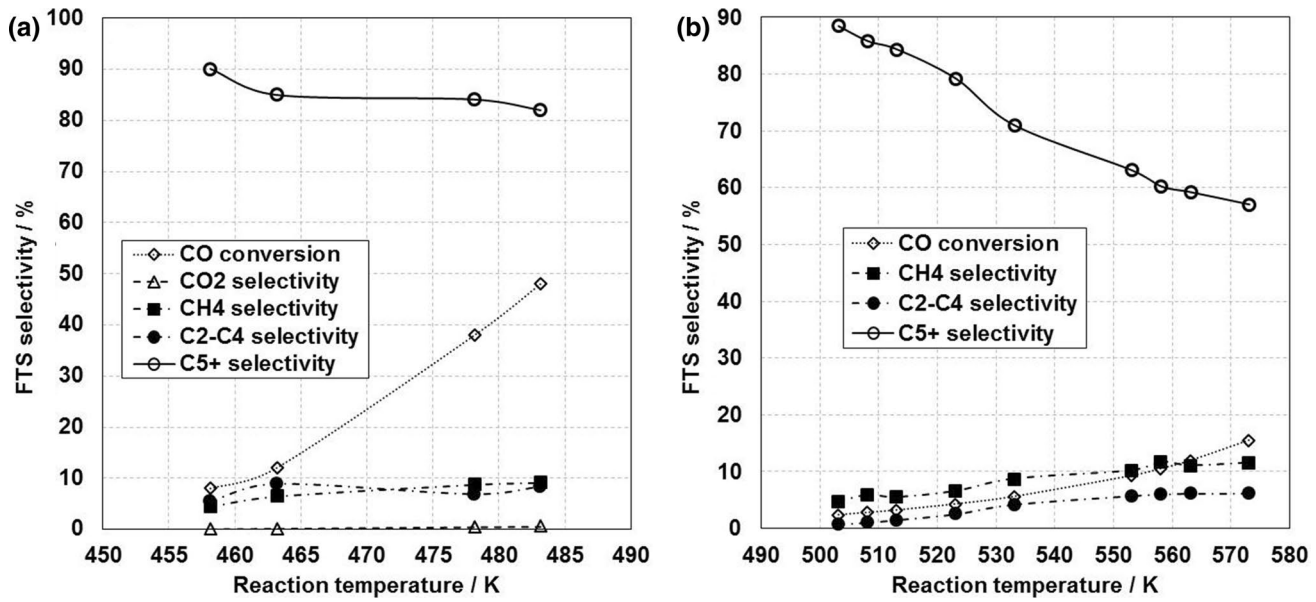

Fig. 19 Effect of reaction conditions on CO conversion and product distribution **a** Co/SiO_2, fixed-bed reactor, H_2:CO = 2, GHSV = 1 $dm^3/g_{cat}/h$; TOS = 100-150 h. Data from [16]. **b** Fixed-bed reactor, H_2:CO = 0.94, GHSV = 4.5 dm^3/gcat/h. Data from [35]

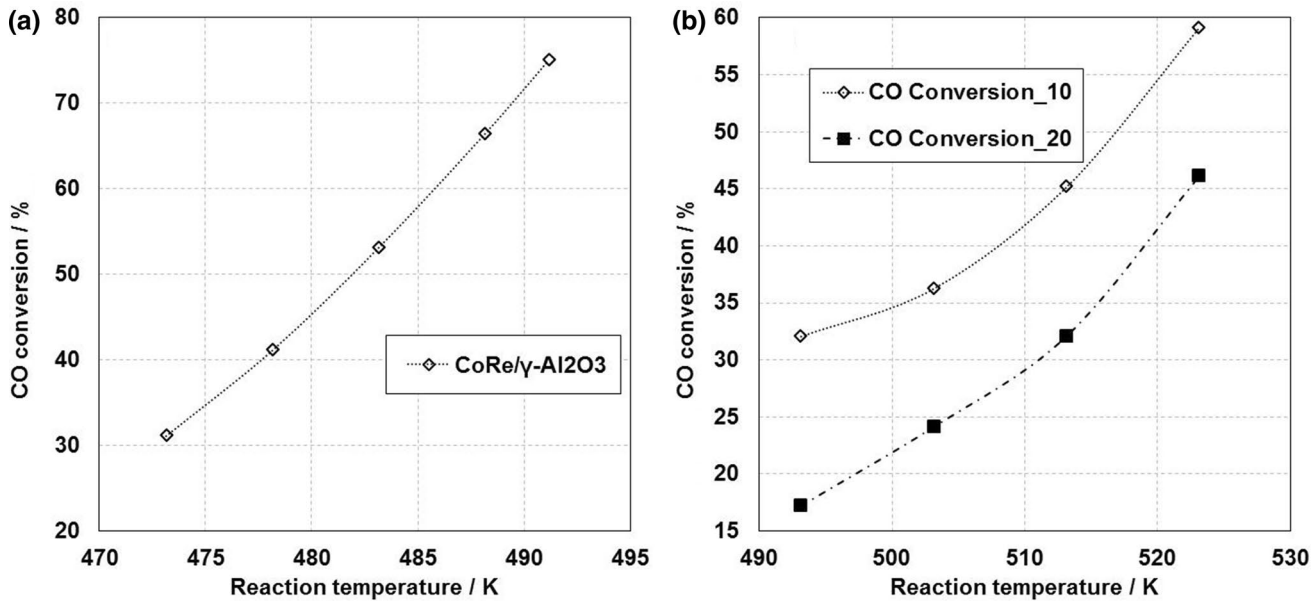

Fig. 20 Effect of reaction temperature on CO conversion over $CoRe/Al_2O_3$ in fixed-bed reactor. **a** 2.35 MPa and over CoPt catalyst in microchannel reactor [72]; **b** 2 MPa, H_2:CO = 2, GHSV 10 and 20 $dm^3/g_{cat}/h$ [70]

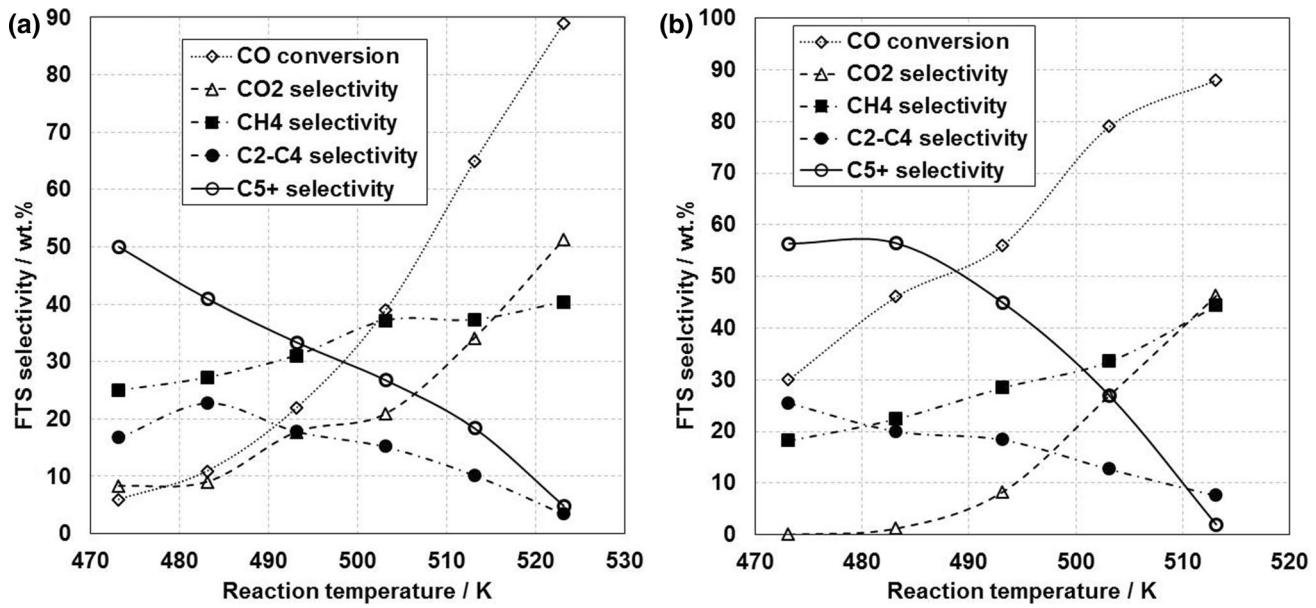

Fig. 21 Effect of reaction temperature on conversion and product distribution over Co/Al_2O_3 (**a**) and Co/ZrO_2 (**b**) in CSTR slurry reactor, 2 MPa. Data from [30]

catalysts, the increase of pressure results in increase of CO conversion and higher selectivity to C_{5+} products (Fig. 25).

The synergy effect of reaction pressure and syngas composition is very important. As will be mentioned later, optimal syngas composition for cobalt-based catalysts is approximately H_2:CO = 2.1 to reduce deactivation rate by coke formation. Figure 26a shows an increase in C_{5+} selectivity as a result of increased reaction pressure when using syngas H_2:CO = 2.1. This is in good agreement with data depicted in Fig. 25. In the case of FTS with H_2:CO reduced to the value of AA, higher pressure results in lower FTS selectivity to C_{5+} products and its

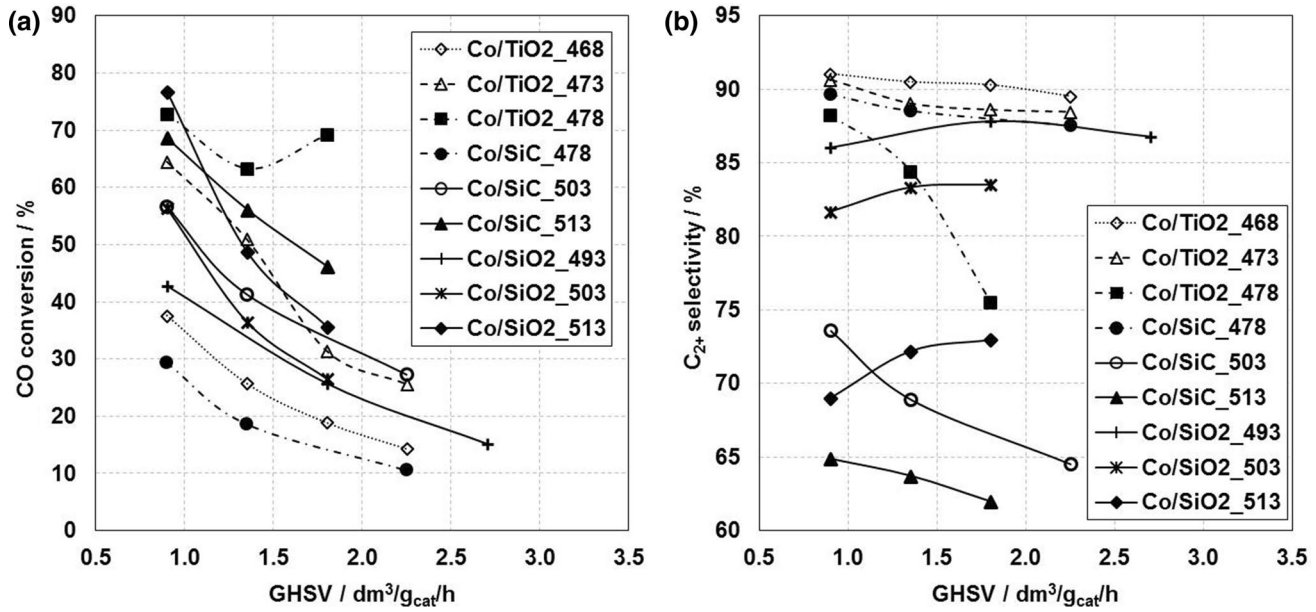

Fig. 22 Effect of GHSV parameter on CO conversion (**a**) and selectivity to C_{2+} products (**b**). Number at the end of catalyst mark refers to reaction temperature in K. Fixed-bed reactor 2 MPa. Data from [29]

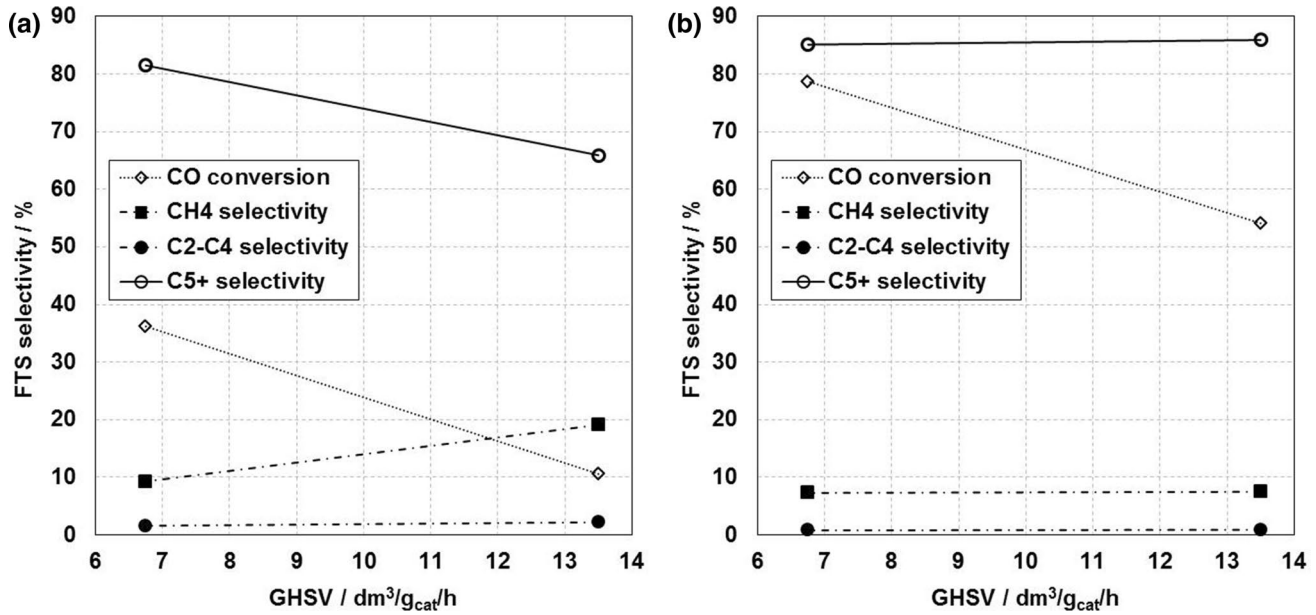

Fig. 23 GHSV effect in CO conversion and products distribution, $CoPt/Al_2O_3$ catalysts 15 (**a**) and 25 wt% (**b**) of Co. H_2:CO = 2, 2 MPa, 493 K. Data from [29]

compensation with higher selectivity to methane and C_2–C_4 products (Fig. 26b).

Iron catalysts

The effect of reaction temperature on FTS catalyzed with iron catalysts is similar as in the case of cobalt catalysts. The only difference is that iron-catalyzed reaction is generally operated at approximately 50 K higher reaction temperatures. Change of reaction temperature from reference value 523–508 K during continuous experiment with commercial catalyst [78] shows significant decrease of CO conversion and little increase of selectivity to CH_4 and C_2–C_4 products. The increase of reaction temperature

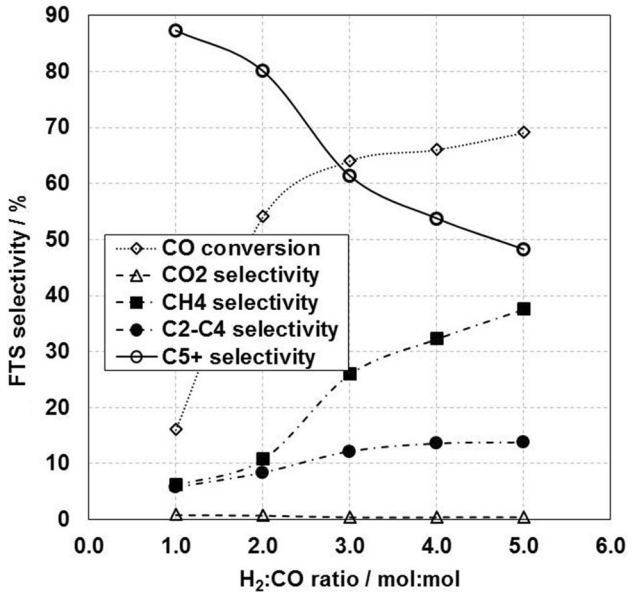

Fig. 24 Effect of syngas composition in FTS; fixed-bed reactor, 487 K, GHSV = 1 $dm^3/g_{cat}/h$, 2 MPa. Data from [16]

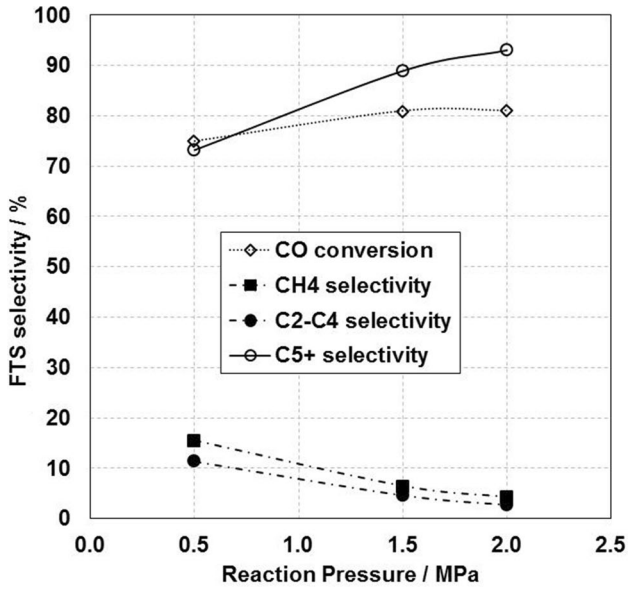

Fig. 25 Effect of reaction pressure of FTS; trickle bed reactor, GHSV = 4.5 $dm^3/g_{cat}/h$, reaction temperature 503.15 K. Data from [34]

from 523 to 538 K increases CO conversion and negatively affects FTS selectivity to C_{5+} products. On the other hand, higher syngas flow rate positively increases FTS selectivity to C_{5+} liquid products but significantly reduces CO conversion. Decrease in CO conversion can be compensated with increase of reaction pressure (changing from 1.5 to 3.0 MPa, Fig. 27). Similarly to cobalt catalysts, increase of H_2:CO ratio evokes higher CO conversion and negatively affects selectivity to C_{5+} liquid products. Selectivity to carbon dioxide raises and declines with changes of CO conversion due to consumption of significant amount of CO by WGS for hydrogen production.

Strong sensitivity of iron catalysts to promoters' content in the composition brings different sensitivity to reaction temperature for catalysts with different promoters. Active carbon supported catalysts promoted with potassium and different amounts of potassium and copper [55] shows all increasing activity and CO conversion, respectively, with raisin reaction temperature from 533 to 563 K. The catalyst without copper promoter was found as more active than catalysts containing copper. On the other hand, higher copper content stabilizes catalysts at reaction temperatures above 543 K and allows to reach higher conversion degrees (Fig. 28a). All the catalysts compared show minimum of selectivity to CH_4 at 543 K. The lowest selectivity to CH_4 was reached with copper-free catalyst (Fig. 28b). The selectivity to C_{5+} products reaches maximum values at 543 K (Fig. 28c) and decreases similarly as described with commercial catalyst (Fig. 27).

Sodium- and sulfur-promoted iron catalyst showed standardly raising CO conversion with increasing reaction temperature and lowering selectivity to liquid products. Opposite to active carbon-supported catalysts, not so significant maximum in CH_4 selectivity was found. The selectivity to methane increases with reaction temperature as well as C_2–C_4 products formation (Fig. 29).

Similar to cobalt catalysts, catalytic activity of iron catalysts can be modified by reaction pressure value. Syngas conversion is significantly raising with pressure increases in all the range of 0.2–2.0 MPa (Figs. 30, 31a, b). The most intensive change in the product composition in the range of 0.2–0.5 MPa. In this pressure range, C_{5+} product selectivity intensively changes with pressure value. Selectivity changes of methane and C_2–C_4 hydrocarbons are not so significant (Fig. 30).

Carbon dioxide selectivity shows stable selectivity from 0.2 to 2.0 MPa reaching values around 47% for iron catalysts with active metal content 10, 20, and 30 wt% (Fig. 30, 31a, 31b). Pressure increase to values higher than 1 MPa shows continuing increase in selectivity of C_{5+} products and syngas conversion. As shown in Fig. 27 (last stage of experiment), pressure change from 1.5 to 3.0 MPa and simultaneous increase of syngas flow rate results in an increase of C_{5+} products selectivity at lower conversion degree. Thus in the case of iron catalysts, reaction pressure can be used to change product selectivity in combination with GHSV to control syngas conversion per pass.

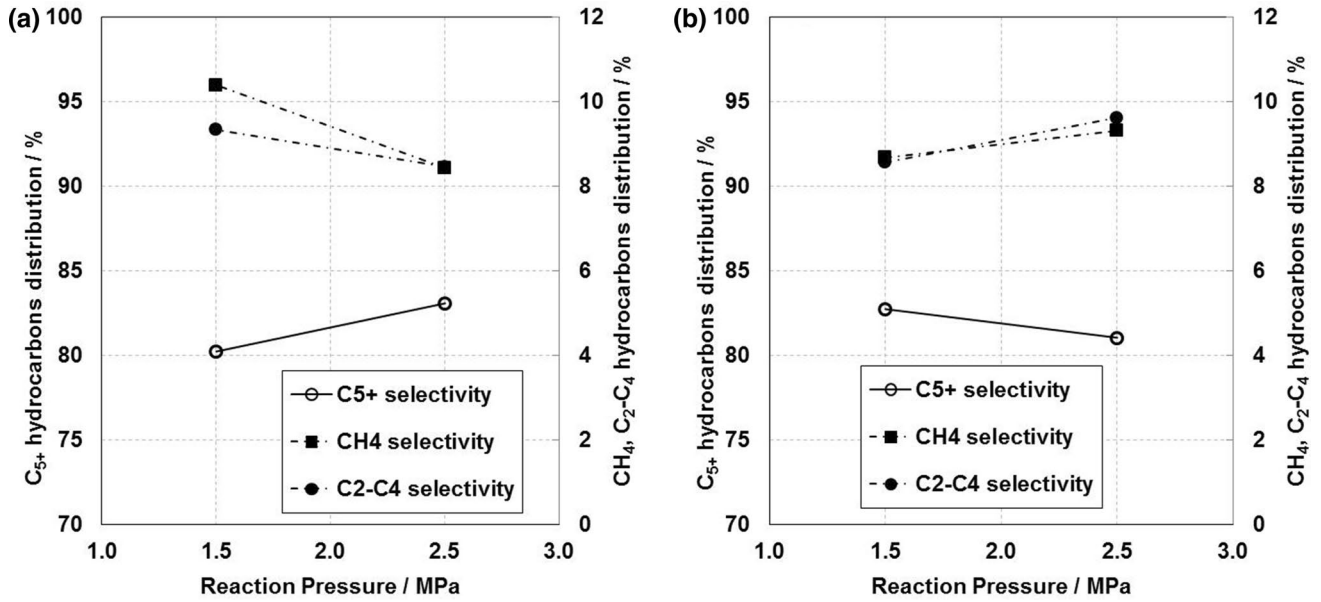

Fig. 26 Effect of reaction pressure of FTS; CSTR slurry reactor, 503.15 K, **a** H_2:CO = 2.1, GHSV = 11.4 $dm^3/g_{cat}/h$; **b** H_2:CO = 1.4, GHSV = 18.1 $dm^3/g_{cat}/h$. Data from [77]

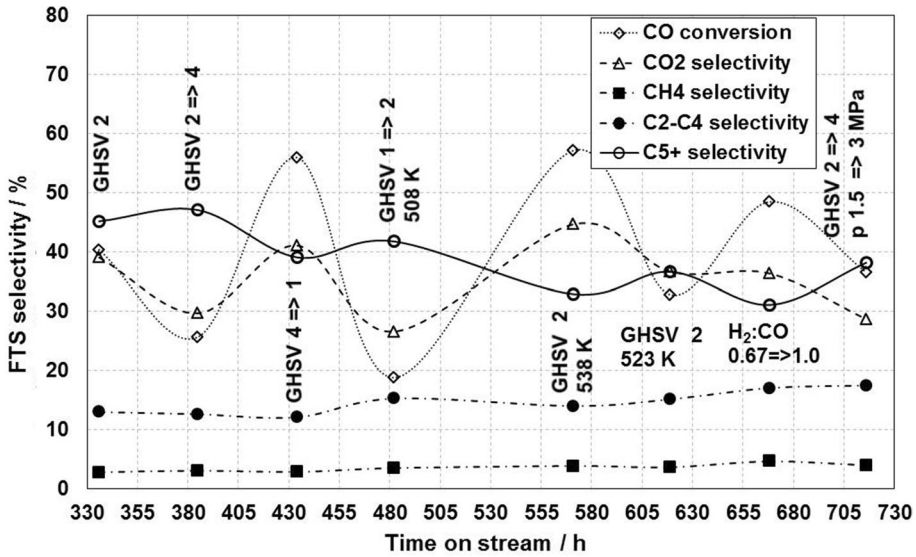

Fig. 27 Effect of reaction conditions changes in fixed-bed reactor with commercial iron FTS catalyst, H_2:CO = 0.67 $dm^3/g_{cat}/h$. Data from [78]

Summary of the role of reaction conditions and catalyst composition

Previous pages showed many ways how to increase FTS activity and to affect products selectivity. Table 1 summarizes basic knowledge about cobalt-based catalysts, Table 2 brings similar summary for Fe-based catalyst.

Catalysts deactivation and inhibitors

FTS operating requires maximizing of catalyst life cycle which is necessary for effective use of the unit. For use of all the catalyst types, fast deactivation can be seen in first hours after process starting followed with continuous and slow catalyst deactivation until the limits of activity degree. Catalyst deactivation can be partially compensated by reaction conditions, such as reaction temperature or GHSV, or by reactivation in the end of life cycle.

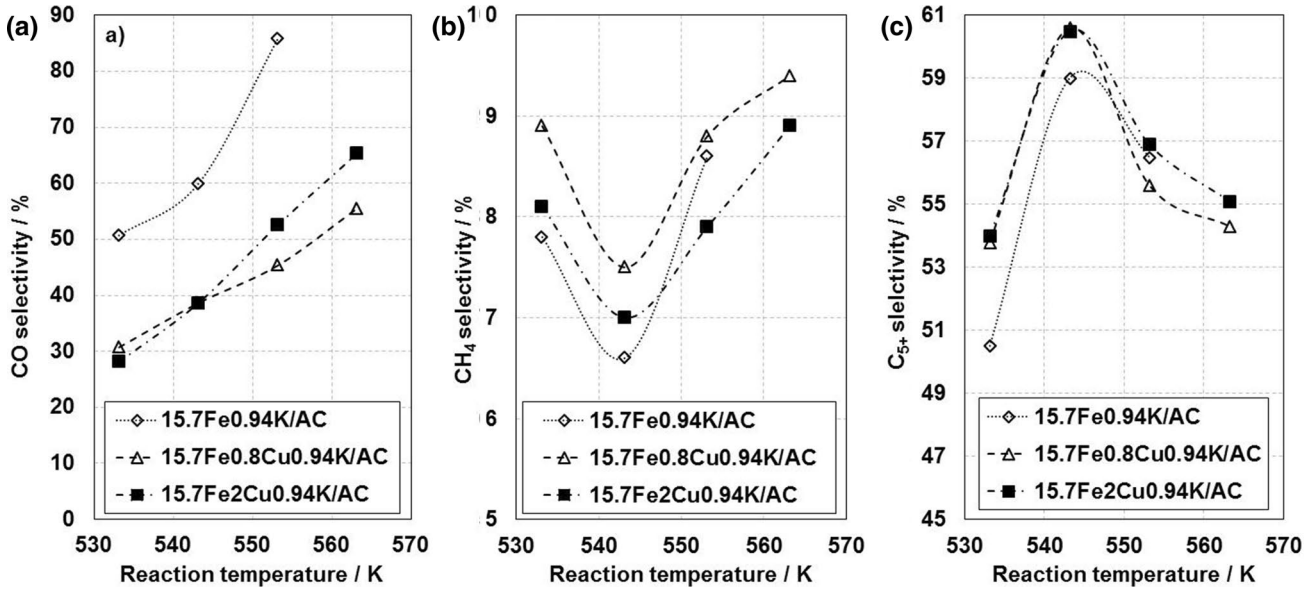

Fig. 28 Effect of reaction temperature on FTS over the Fe/AC catalysts; fixed-bed reactor, 2.07 MPa, GHSV = 3 $dm^3/g_{cat}/h$, H_2:CO = 0.9. Data from [55]

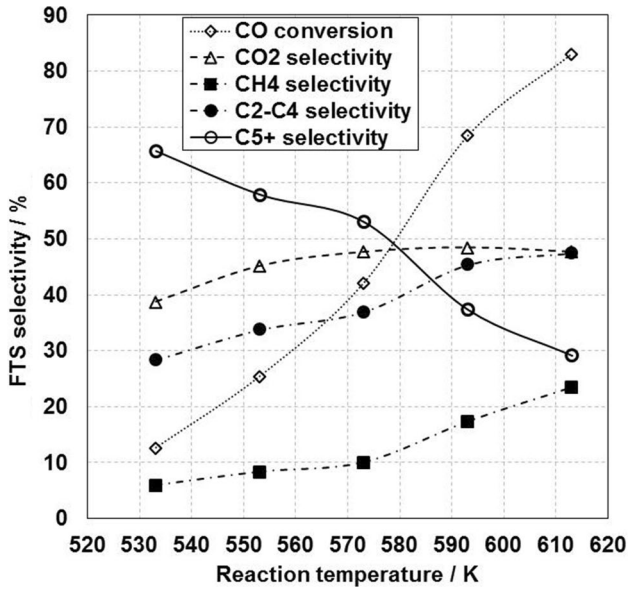

Fig. 29 Effect of reaction temperature on FTS over the 10Fe0.8Na0.1S/SiC; fixed-bed reactor, H_2:CO = 1.1, 1 MPa, GHSV = 2.2 $dm^3/g_{cat}/h$. Data from [39]

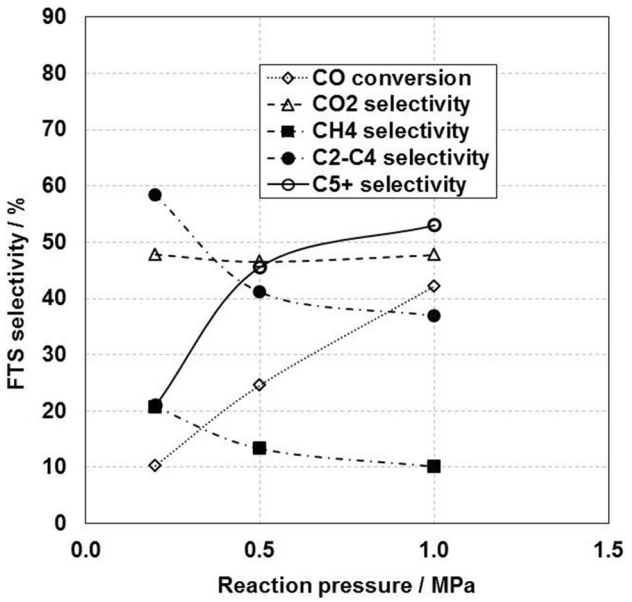

Fig. 30 Effect of reaction pressure of FTS; fixed-bed reactor, - K, GHSV = 2.2 $dm^3/g_{cat}/h$, H_2:CO = 1.1; reaction temperature 573.15 K; 10 wt% Fe. Data from [39]

Cobalt catalysts

The main causes of catalyst deactivation are sintering of reduced cobalt phase and its reoxidation and formation of carbon deposits. These phenomena occur simultaneously; nevertheless they can be sorted based on reaction rate. Active phase sintering is the fastest deactivation pathway and it occurs in the initial stages of reaction in first dozens of hours on stream [79]. Moreover, sintering is accelerated by the presence of water and its partial pressure increase, respectively [80]. In this case, the water incoming to the reactor as moisture in syngas and the water formed during FTS have both the same effect to active phase sintering. On the other hand, formation of carbon deposits is significantly slower than sintering. The effect of this deactivation pathway occurs after longer time period of TOS of the run

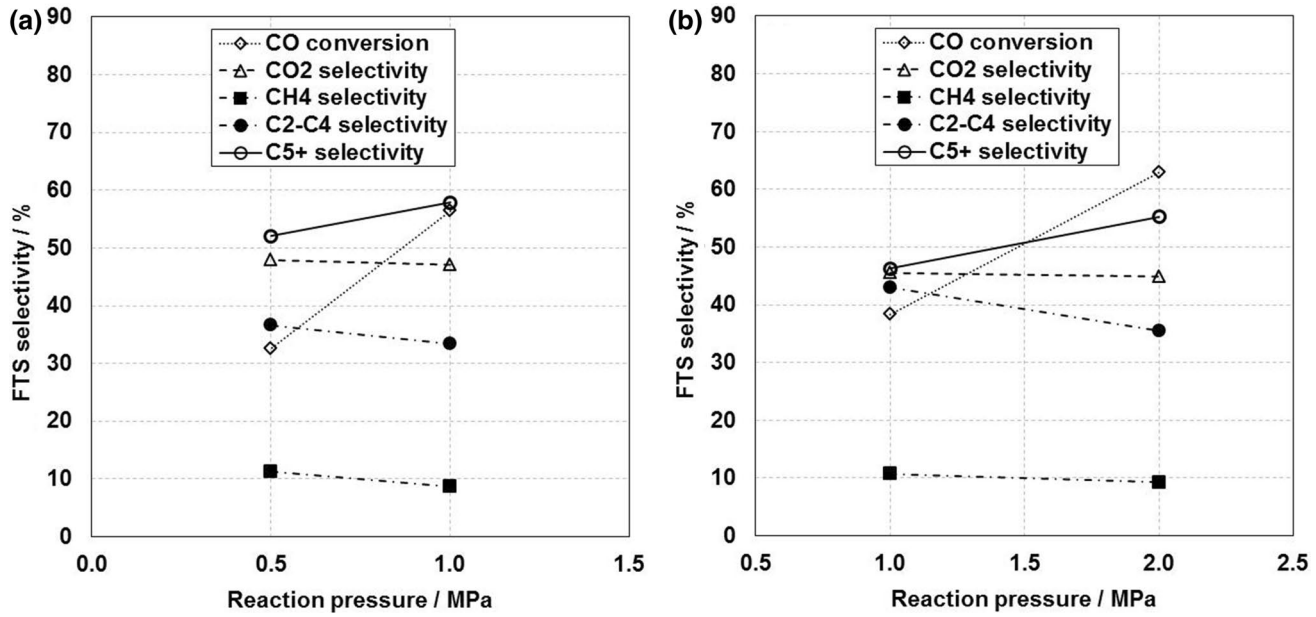

Fig. 31 Effect of reaction pressure of FTS; fixed-bed reactor, GHSV = 2.2 $dm^3/g_{cat}/h$, H_2:CO = 1.1; reaction temperature 573.15 K; **a** 20 wt% Fe; **b** 30 wt% Fe. Data from [39]

Table 1 Summary for Co catalysts, reaction conditions, promoters, and catalyst support

Parameter	Effect
Reaction temperature	Raising temperature increases catalyst activity and reduces C_{2+} selectivity
Reaction pressure	Raising pressure results in higher conversion and C_{5+} selectivity, low H_2:CO (below 2) reduces C_{5+} selectivity
GHSV	Higher GHSV results in lower CO conversion and little lower C_{2+} selectivity
H_2:CO ratio	Increase in ratio results in higher CO conversion, the most significant between values 1–2, increases C_{5+} selectivity
Promoters	
Pt, Ru, Re, Ag, Rh	Lowering of reduction/activation temperature
Ru	Increase in CO conversion higher C_{5+} selectivity
Pt, Re, Ru	Increase in catalytic activity (Co/Al_2O_3)
Ru + Pt	Increase in activity and slower reoxidation
Zr	Higher yield of C_{5+} products, inhibition of WGS and methanation
Catalyst supports	
Al_2O_3	The most common, strong effect of active metal loading, organic solutions are promoting final FTS activity
SiO_2	Higher FTS activity and C_{5+} selectivity
ZSM-5	Increase of deactivation rate with raising mesopore volume
Y-zeolite	Mesopore presence reduces CO conversion

[79]. Cobalt phase reoxidation rate significantly depends on water partial pressure in the system and exceeding of limit values (depending on other reaction parameters) results in significant acceleration of cobalt reoxidation. Deactivation by reoxidation can be identified by increase of selectivity to CH_4 formation [63] and in the case of Al_2O_3 supported catalysts the reoxidation is accompanied by formation of inactive $xCoO{\cdot}yAl_2O_3$ phases [81]. The comparison of CNT and Al_2O_3 supported catalysts shows less significant cobalt phase sintering into larger particles on Al_2O_3 support. Formation of carbon deposits is caused by polymerization of reaction intermediates on the catalyst surface on both, the surface of active phase and the catalyst support as well. Carbon deposits located on the surface of catalyst support are more stable and more resistant to reduction [66]. Carbon deposits can be sorted into three groups: hydrocarbons (i), strongly adsorbed alkanic hydrocarbons (ii), and amorphous polymeric carbon (iii) [67]. Distribution of deposits types on the catalyst surface strongly depends on operating regime. Proceeding

Table 2 Summary for Fe catalysts, reaction conditions, promoters, and catalyst support

Parameter	Effect
Reaction temperature	Raising temperature increases catalyst activity and reduces C_{2+} products selectivity; max. C_{5+} selectivity at approx. 540 K
Reaction pressure	Increase of pressure increases CO conversion and C_{5+} selectivity
GHSV	Raising value reduces CO conversion and increases C_{5+} selectivity
H_2:CO ratio	Ratio increase increases CO conversion and C_2–C_4 selectivity
Promoters	
Na, K	Lower catalytic ability, higher catalyst stability
K	Higher C_{5+} selectivity, to be used for SiO2 supported catalysts
Na	Higher C_{5+} selectivity, to be used for SiC supported catalysts
S (Na)	Affects CO conversion, decreasing C_{5+} selectivity with raising reaction temperature
S	Lower coverage of active particles with hydrogen
Cu	Simpler Fe reduction, lower FTS and WGS activity, higher C_{5+} selectivity
MgO (Cu)	Fe particle stabilization, avoids sintering, smaller crystallites, higher activity
Mn	Higher FTS activity, high selectivity to C_2–C_4 products
Zr	Inhibition of reduction and carburization
Ni	Higher activity and lower C_{5+} selectivity
Catalyst supports	
TiO_2 > active carbon > SiC > SiO_2 > Al_2O_3	Order of FTS activity based on catalyst support

of syngas with CO rich syngas with H_2:CO ratio lower than 2 with medium conversion degree results in slow deactivation by deposition of mainly strongly adsorbed hydrocarbons and polymeric carbon. Combination of low H_2:CO ratio with low GHSV results in faster deposition of carbonaceous species on the catalyst surface. The most intensive in that case is deposition of strongly adsorbed hydrocarbons and amorphous polymeric carbon [67].

Deactivation of cobalt catalysts in industrial scale takes place typically in non-standard states of the run, such as start-up and shut-down of the process, when the catalyst can be exposed to undesirable reaction conditions [82]. During these operations the catalyst can be exposed to the catalytic poisons incoming to the catalyst bed because of improper work of syngas pre-treating. These impurities are sulfane [65, 83], ammonia [84], and other nitrogen-containing compounds [27, 85], hydrogen halides, and tars.

Iron catalysts

Similarly to cobalt catalysts, iron catalysts are deactivated by active phase reoxidation (i), carbon deposition (ii), and in the case of supported catalysts by releasing of active metal from catalyst particles (iii). Iron reoxidation can be limited by operating FTS with lower conversion and lower water vapor partial pressure, respectively [86]. Another way to decrease the deactivation rate by reoxidation is application of promoters of active metal, namely potassium [41]. Formation of carbon deposits reduces catalyst activity by blocking of mass transport to and from active sites. The surface of alkaline promoted can be covered by plenty of types of carbonaceous species, and these are sorted by reducibility by hydrogen to (i) adsorbed atomic carbon, (ii) amorphous slightly polymeric hydrocarbon or carbon surface compounds, (iii) large carbide particles, and (iv) disordered and partially ordered graphite-like surface compounds. Despite increase of surface basicity of iron catalysts, CO dissociation is faster than carbon hydrogenation. This results in deposition of surplus carbon and in the formation of inactive carbide phases and graphite surface compounds. These cause the catalyst deactivation [42].

Similar to cobalt catalysts, besides deactivation pathways specific for iron catalysts, deactivation takes place as an effect of catalytic poisons from syngas. These are sulfane [87], carbonylsulfide, ammonia [27, 88], and hydrogen halides [89].

Reactors for FTS

Intended or available technology design rules in catalyst selection and operating conditions. Common and traditional are tubular reactors with fixed-bed of catalyst (and its modification—trickle bed), bubble column reactors, and CSTR and slurry reactors and microchannel reactors. Due to intensive heat formation during FTS, all the reactor designs are similar to industrially used heat exchangers using an external coolant to keep reaction at required temperature or

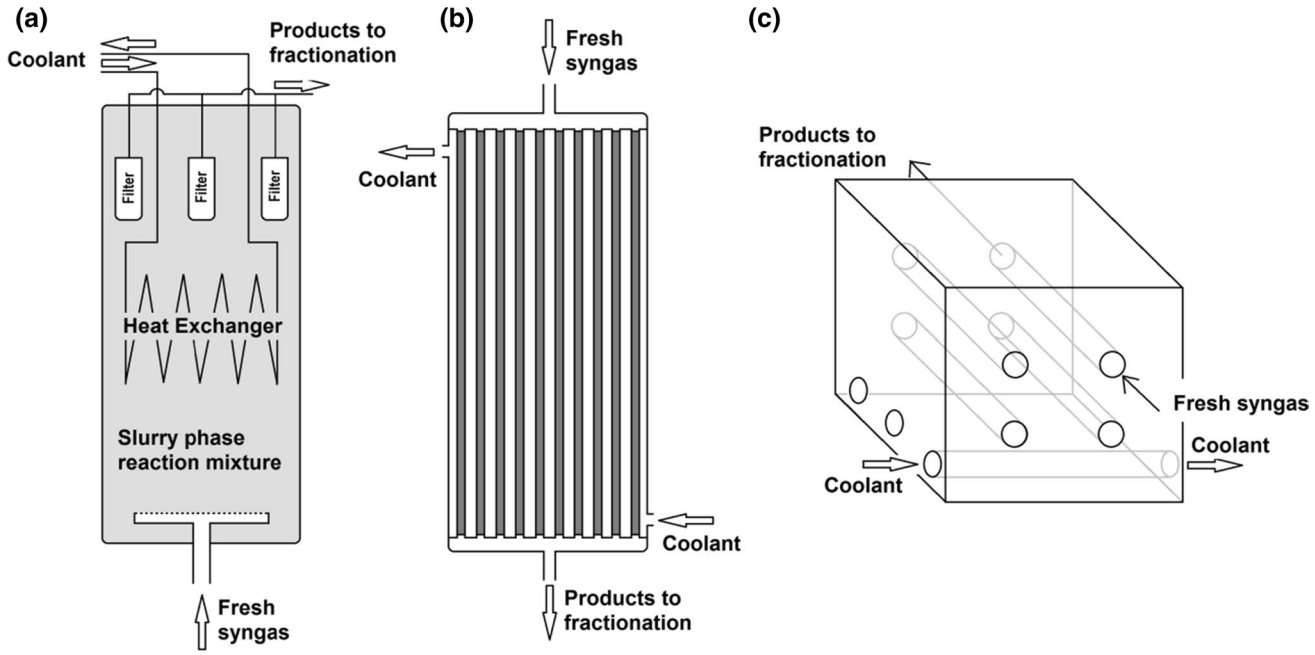

Fig. 32 Schematic drawing of basic types of FTS reactors, **a** slurry reactor; **b** fixed-bed reactor; **c** microchannel reactor

temperature interval, respectively. The schematic drawing of basic reactor types is shown in Fig. 32.

Fixed bed reactors

These reactors are the simpler concept of reactor. Catalyst particles with size in units of millimeters are loaded inside inner reactor tube. This tube is typically placed in another tube with heat exchange liquid (construction of duplicator). In the beginning of the process, duplicator serves for introduction of heat into the system, while during the process it removes reaction heat from the system to avoid reactor overheating and uncontrolled reaction run (pilot units, lab-scale reactors). High value of the FTS heat of reaction puts high requirement for maximizing of heat removal for efficient run of the reactor. This is usually reached by use of optimal ratio of catalyst bed volume and heat exchange area of the reactor. This results in application of tubular reactors in configuration of multitubular reactor (several thousand tubes) placed in duplicator. Duplicator is usually filled with coolant, which is cooled outside the reactor. Coolant is usually thermo-oil, water or boiling water that increases cooling effect with heat of vaporization.

Fixed bed of catalyst is specific for FTS operating, because the limiting factor of the system is rate of heat removal. This parameter determines maximal syngas conversion by one pass through the reactor to 30–50%. This means that for effectivity and economy of the process the unreacted syngas has to be recirculated together with make-up syngas in the reactor. Make-up flow rate in steady state is given by syngas conversion/consumption. Fixed bed reactors are operated with high temperature difference between inlet and outlet of catalyst layer. This difference reaches tenths of Kelvins and results in different deactivation rates along the catalyst bed because of different reaction temperatures and exposure to reaction mixture with different composition, especially different water vapor partial pressure, especially in the end of catalyst bed with combination of high temperature and high water vapor partial pressure. To reduce deactivation rate, recycle of unreacted syngas and part of light products can be used. Moreover, light products with boiling point up to 473 K contains relatively high content of olefins, which can continue to react in FTS and increase the process selectivity to heavier products.

Thanks to its construction, fixed-bed reactors can be theoretically operated at higher temperature than slurry reactors. This makes this type of reactor suitable for both catalyst types—cobalt- and iron-based catalysts. Typical behavior for these reactors is the high pressure drop in catalyst bed, which is given by volume contraction during hydrocarbon chain formation [90].

Slurry phase reactors

Unlike fixed-bed reactors, smaller catalyst particles are used in slurry reactors. Catalyst is dispersed in reaction mixture and held in suspension by circulation of reaction mixture, by stirring (CSTR slurry phase reactors, usually lab-scale), or/and by syngas incoming to the bottom of the reactor through

the semi-permeable membrane. Rate determining step of slurry phase systems is the mass transport of reactants to/from active sites.

This reactor type is based on one reactor vessel with integrated heat exchanger, because the reactor is just one vessel with larger volume than in case of fixed-bed reactors. Slurry reactors are almost exclusively used in combination with cobalt-based catalysts. Catalyst is used in the form of powder with particle size in the range of approximately 10–100 μm. It is result of need of keeping the catalyst dispersed in reaction mixture and to avoid catalyst sedimentation. As the catalyst is dispersed in the reactor, products must be removed from the reactor by filtering. Intensive moving of catalyst particles in the reactors brings the problem with catalyst attrition resulting in higher requirements for catalyst mechanical stability. In comparison with fixed-bed reactors, slurry reactors are able to reach lower temperature diferences along the reactor [90].

Microchannel reactors

Microchannel reactor is the newest and the most investigated reactor design of the presence. These reactors represent optimization in the field of reaction temperature control and in the field of diffusion as well. The reactor design is based on two independent microchannel systems in metallic block with channel size in units of millimeters. Catalyst is placed in reactor channels and is loaded on the inner wall of channels. The active phase is usually cobalt based. Coolant (thermo-oil, water, boiling water) is pumped in the cooling channels. Both channel systems are usually oriented in parallel (concurrent or contradictory flow possible), in cross or with "U" shape channels [91]. For a simple imagination, construction of these reactors could be described as similar to design of block heat exchangers with catalyst in one of channel system.

As mentioned above, microchannel reactors allow very well to control the reaction temperature and with temperature difference (inlet to outlet) in units of K [92].

Alternative designs of reactors

Mathematical simulations and modelling allow to study innovative designs of reactors without need of construction of experimental or pilot unit. One of the ideas is to remove reaction heat of FTS by another endothermic reaction directly in duplicator (instead of coolant circulation) [93]. Another reactor design is based on two-stage catalytic system with semi-permeable membranes passing contradictory through the reactors and introducing syngas to the system with hydrogen dosing into the system along the semi-permeable system [94].

Sophisticated controlling systems and high investment costs of reactor designs like these makes it difficult to implement them in the near future.

Materials and methods

Publications with numerically presented results served as source data for description of FTS based on catalysts type, promoters used for catalysts modifications and optimization and based on reaction conditions. No data from charts were used for this purpose. Due to variety of reaction conditions for experiments in published papers, these vary in this work as well and are always described in each case, typically under figures. Typical parameters discussed in most of the figures are syngas conversion and selectivity to CO_2, CH_4, C_2–C_4 hydrocarbons, and C_{5+} hydrocarbons. Due to significantly different way of data analysis by authors, most of the data were recalculated to make the final text more unified.

Conclusions

Cobalt- and iron-based FTS catalysts both have many possibilities how to be used and optimized for required hydrocarbons' production. Cobalt-based low-temperature catalysts can be modified by noble metals, such as Ru and Pt to be more stable and to gain higher FTS activity (Pt, Ru, Re, Rh, Ag). The method of cobalt precursors loading into catalyst plays an important role in catalyst activity. Catalyst support selection, and its pore volume or solvent selection, all of these parameters affect behavior of the catalyst in FTS. The most commonly used alumina supports do not offer the highest activity, but their properties are very well known and bring many opportunities for properties modifications.

High-temperature iron catalyst can be optimized in the same way as cobalt types. Typical alkali metals (K, Na) are used together with copper or sulfur to stabilize the catalyst and to increase liquid products' selectivity. Conversion can be increased in both cases by increase of reaction temperature, syngas flow rate decrease, and pressure increase.

Acknowledgements This publication is a result of the project CATAMARAN, Reg. no. CZ.02.1.01/0.0/0.0/16_013/0001801, which has been co-financed by European Union from the European Regional Development Fund through the Operational Programme Research, Development and Education. This project has also been financially supported by the Ministry of Industry and Trade of the Czech Republic which has been providing institutional support for long-term conceptual development of research organisation. The project CATAMARAN has been integrated into the National Sustainability Programme I of the Ministry of Education, Youth and Sports of the Czech Republic (MEYS) through the project Development of the UniCRE Centre (LO1606).

References

1. Elliott D, Hart T, Neuenschwander G, Rotness L, Zacher A (2009) Environ Prog Sustain Energy 28:441
2. Elliott D, Hart T, Neuenschwander G, Rotness L, Olarte M, Zacher A, Solantausta Y (2012) Energy Fuels 26:3891
3. Olarte M, Zacher A, Padmaperuma A, Burton S, Job H, Lemmon T, Swita M, Rotness L, Neuenschwander G, Frye J, Elliott D (2016) Top Catal 59:55
4. Horáček J, Kubička D (2017) Fuel 198:49
5. Al-Dossary M, Fierro JLG (2015) Appl Catal A 499:109
6. Hu J, Yu F, Lu Y (2012) Catalysts 2:303
7. Takahara I, Murata K, Sato K, Miura Y, Inaba M, Liu Y (2013) Appl Catal A 450:80
8. Liu L, Sun G, Wang C, Yang J, Xiao C, Wang H, Ma D, Kou Y (2012) Catal Today 183:136
9. Nurunnabi M, Murata K, Okabe K, Hanaoka T, Miyazawa T, Sakanishi K (2010) J Jpn Pet Inst 53:75
10. Takahara I, Murata K, Sato K, Inaba M, Liu Y (2014) Appl Catal A 482:205
11. Ma W, Jacobs G, Keogh RA, Bukur DG, Davis BH (2012) Appl Catal A 437–438:1
12. Ma W, Jacobs G, Pendyala VRR, Sparks DE, Shafer WD, Thomas GA, MacLennan A, Hu Y, Davis BH (2018) Catal Today 299:28
13. Pardo-Tarifa F, Cabrera S, Sanchez-Dominguez M, Boutonnet M (2017) Int J Hydrogen Energy 42:9754
14. Phaahlamohlaka TN, Dlamini MW, Mogodi MW, Kumi DO, Jewell LL, Billing DG, Coville NJ (2018) Appl Catal A 552:129
15. Shimura K, Miyazawa T, Hanaoka T, Hirata S (2014) J Mol Catal A Chem 394:22
16. Savost'yanov AP, Yakovenko RE, Narochniy GB, Sulima SI, Bakun VG, Soromotin VN, Mitchenko SA (2017) Catal Commun 99:25
17. Vosoughi V, Badoga S, Dalai AK, Abatzoglou N (2017) Fuel Process Technol 162:55
18. Cheng K, Subramanian V, Carvalho A, Ordomsky VV, Wang Y, Khodakov AY (2016) J Catal 337:260
19. Coronel-García MA, Reyes de la Torre AI, Melo-Banda JA, Martínez-Salazar AL, Rodrigo RS, Díaz Zavala NP, Portales Martínez B, Domínguez JM (2015) Int J Hydrogen Energy 40:17264
20. Tavasoli A, Trépanier M, Abbaslou RMM, Dalai AK, Abatzoglou N (2009) Fuel Process Technol 90:1486
21. Bertella F, Concepción P, Martínez A (2017) Catal Today 289:181
22. Aluha J, Abatzoglou N (2016) Biomass Bioenergy 95:330
23. Jian-Kang H, Li-Tao J, Bo H, De-Bao L, Yan L, Ya-Chun L (2015) J Fuel Chem Technol 43:846
24. Ghasvareh P, Smith KJ (2016) Energy Fuels 30:9721
25. Jang IH, Um SH, Lim B, Woo MH, Jun KW, Lee JB, Bae JW (2013) Appl Catal A 450:88
26. Ma W, Jacobs G, Gao P, Jermwongratanachai T, Shafer WD, Pendyala VRR, Yen CH, Klettlinger JLS, Davis BH (2014) Appl Catal A 475:314
27. Ordomsky VV, Carvalho A, Legras B, Paul S, Virginie M, Sushkevich VL, Khodakov AY (2016) Catal Today 275:84
28. Sun Y, Yang G, Sun G, Sun Z, Zhang L (2017) Environ Prog Sustainable Energy 37:553
29. Zhu X, Lu X, Liu X, Hildebrandt D, Glasser D (2014) Chem Eng J 247:75
30. Kulikova MV, Dement'eva OS, Kuz'min AE, Chudakova MV (2016) Pet Chem 56:1140
31. Rodrigues JJ, Pecchi G, Fernandes FAN, Rodrigues MGF (2012) J Nat Gas Chem 21:722
32. Liao P, Zhang C, Zhang L, Yang Y, Zhong L, Wang H, Sun Y (2018) Catal Today 311:56
33. Kang J, Wang X, Peng X, Yang Y, Cheng K, Zhang Q, Wang Y (2016) Ind Eng Chem Res 55:13008
34. Nishizawa A, Kitanom T, Ikenaga N, Miyake T, Suzuki T (2014) J Jpn Pet Inst 57:109
35. Zohdi-Fasaei H, Atashi H, Tabrizi FF, Mirzaei AA (2016) J Nat Gas Sci Eng 32:262
36. Comazzi A, Pirola C, Longhi M, Bianchi CLM, Suslick KS (2017) Ultrason Sonochem 34:774
37. Blanchard J, Abatzoglou N (2014) Catal Today 237:150
38. Chalupka KA, Maniukiewicz W, Mierczynski P, Maniecki T, Rynkowski J, Dzwigaj S (2015) Catal Today 257:117
39. Feng Jiang F, Zhang M, Liu B, Xu Y, Liu X (2017) Catal Sci Technol 7:1245
40. Qian W, Zhang H, Sun Q, Liu Y, Ying W, Fang D (2014) React Kinet. Mech Catal 111:293
41. Pendyala VRR, Graham UM, Jacobs G, Hamdeh HH, Davis BH (2014) Catal Lett 144:1704
42. Pour AN, Housaindokht MR, Zarkesh J, Tayyari SF (2010) J Ind Eng Chem 16:1025
43. Geng S, Jiang F, Xu Y, Liu X (2016) ChemCatChem Commun 8:1303
44. Kang SW, Bae JW, Cheon JY, Lee YJ, Ha KS, Jun KW, Lee DH, Kim BW (2011) Appl Catal B 103:169
45. Jermwongratanachai T, Jacobs G, Shafer WD, Pendyala VRR, Ma W, Gnanamani MK, Hopps S, Thomas GA, Kitiyanan B, Khalid S, Davis BH (2014) Catal Today 228:15
46. Kungurova OA, Khassin AA, Cherepanova SV, Saraev AA, Kaichev VV, Shtertser NV, Chermashentseva GK, Gerasimov EU, Paukshtis EA, Vodyankina OV, Minyukova TP, Abou-Jaoudé G (2017) Appl Catal A 539:48
47. Cook KM, Samiksha Poudya S, Miller JT, Bartholomew CH, Hecker WC (2012) Appl Catal A 449:69
48. Cook KM, Perez HD, Bartholomew CH, Hecker WC (2014) Appl Catal A 482:275
49. Jacobs G, Patterson PM, Zhang Y, Das T, Li J, Davis BH (2002) Appl Catal A 233:215
50. Park SJ, Bae JW, Lee YJ, Ha KS, Jun KW, Karandikar P (2011) Catal Commun 12:539
51. Cano LA, Garcia Blanco AA, Lener G, Marchetti SG, Sapag K (2017) Catal Today 282:204
52. Galvis HMT, Koeken ACJ, Bitter JH, Davidian T, Ruitenbeek M, Dugulan AI, de Jong KP (2013) J Catal 303:22
53. Xie J, Yang J, Dugulan AI, Holmen A, Chen D, de Jong KP, Louwerse MJ (2016) ACS Catal 6:3147
54. Al-Dossary M, Fierro JLG, Spivey JJ (2015) Ind Eng Chem Res 54:911
55. Ma W, Kugler EL, Dadyburjor DB (2011) Energy Fuels 25:1931
56. Pendyala VRR, Jacobs G, Gnanamani MK, Hu Y, MacLennan A, Davis BH (2015) Appl Catal A 495:45
57. Campos A, Lohitharn N, Roy A, Lotero E, Goodwin JG Jr, Spivey JJ (2010) Appl Catal A 375:12
58. Liu Y, Chen JF, Bao J, Zhang Y (2015) ACS Catal 5:3905
59. Zhang Y, Ma L, Wang T, Li X (2016) Fuel 177:197
60. Ahn CI, Bae JW (2016) Catal Today 265:27
61. Mosayebi A, Mehrpouya MA, Abedini R (2016) Chem Eng J 286:416
62. Kim SM, Bae JW, Lee YJ, Jun KW (2008) Catal Commun 9:2269
63. Lancelot C, Ordomsky VV, Stéphan O, Sadeqzadeh M, Karaca H, Lacroix M, Curulla-Ferré D, Luck F, Fongarland P, Griboval-Constant A, Khodakov AY (2014) ACS Catal 4:4510
64. Ma W, Jacobs G, Das TK, Masuku CM, Kang J, Pendyala VRR, Davis BH (2014) Ind Eng Chem Res 53:2157
65. Ma W, Jacobs G, Shafer WD, Pendyala VRR, Xiao Q, Hu Y, Davis BH (2016) Catal Lett 146:1204

66. Peña D, Griboval-Constant A, Lancelot C, Quijada M, Visez N, Stéphan O, Lecocq V, Diehl F, Khodakov AY (2014) Catal Today 228:65
67. Peña D, Griboval-Constant A, Lecocq V, Diehl F, Khodakov AY (2013) Catal Today 215:43
68. Rohani AA, Khorashe F, Safekordi AA, Tavassoli A (2010) Pet Sci Technol 28:458
69. Rai A, Sibi MG, Farooqui SA, Anand M, Bhaumik A, Sinha AK (2017) ACS Sustainable Chem Eng 5:7576
70. Shin MS, Park N, Park MJ, Cheon JY, Kang JK, Jun KW, Ha KS (2014) Fuel Process Technol 118:235
71. Holmen A, Venvik HJ, Myrstad R, Zhu J, Chen D (2013) Catal Today 216:150
72. Knochen J, Güttel R, Knobloch C, Turek T (2010) Chem Eng Process 49:958
73. Wei L, Zhao Y, Zhang Y, Liu C, Hong J, Xiong H, Li J (2016) J Catal 340:205
74. Wang Y, Jiang Y, Huang J, Liang J, Wang H, Li Z, Wu J, Li M, Zhao Y, Niu J (2016) Fuel 174:17
75. Bertella F, Concepción P, Martínez A (2017) Catal Today 296:170
76. Cheng K, Ordomsky VV, Legras B, Virginie M, Paul S, Wang Y, Khodakov AY (2015) Appl Catal A 502:204
77. Todic B, Ma W, Jacobs G, Davis BH, Bukur DB (2014) J Catal 311:325
78. Bukur DB, Patel SA, Lang X (1990) Appl Catal 61:329
79. Sadeqzadeh M, Chambrey S, Hong J, Fongarland P, Luck F, Curulla-Ferré D, Schweich D, Bousquet J, Khodakov AY (2014) Ind Eng Chem Res 53:6913
80. Sadeqzadeh M, Chambrey S, Piché S, Fongarland P, Luck F, Curulla-Ferré D, Schweich D, Bousquet J, Khodakov AY (2013) Catal Today 215:52
81. Tavasoli A, Karimi S, Taghavi S, Zolfaghari Z, Amirfirouzkouhi H (2012) J Nat Gas Chem 21:605
82. Rytter E, Holmen A (2015) Catalysts 5:478
83. Pansare SS, Allison JD (2010) Appl Catal A 387:224
84. Pendyala VRR, Jacobs G, Bertaux C, Khalid S, Davis BH (2016) J Catal 337:80
85. Pendyala VRR, Gnanamani MK, Jacobs G, Ma W, Shafer WD, Davis BH (2013) Appl Catal A 468:38
86. Sehabiague L, Basha OM, Hong Y, Morsi B, Shi Z, Jia H, Weng L, Men Z, Liu K, Cheng Y (2015) AIChE J 61:3838
87. Ma W, Jacobs G, Sparks DE, Shafer WD, Hamdeh HH, Hopps SD, Pendyalaa VRR, Hu Y, Xiao Q, Davis BH (2016) Appl Catal A 513:127
88. Ma W, Jacobs G, Sparks DE, Pendyala VRR, Hopps SG, Thomas GA, Hamdeh HH, MacLennan A, Hu Y, Davis BH (2015) J Catal 326:149
89. Ma W, Jacobs G, Thomas GA, Shafer WD, Sparks DE, Hamdeh HH, Davis BH (2015) ACS Catal 5:3124
90. Boyer C, Gazarian J, Lecocq V, Maury S, Forret A, Schweitzer JM, Souchon V (2016) Oil Gas Sci Technol 71:44
91. Jung I, Kshetrimayum KS, Park S, Na J, Lee Y, An J, Park S, Lee CJ, Han C (2016) Ind Eng Chem Res 55:505
92. Sun Y, Jia Z, Yang G, Zhang L, Sun Z (2017) Int J Hydrogen Energy 42:29222
93. Rahimpour MR, Khademi MH, Bahmanpour AM (2010) Chem Eng Sci 65:6206
94. Rahimpour MR, Forghani AA, Khosravanipour Mostafazadeh A, Shariati A (2010) Fuel Process Technol 91:33